Gene expression profiling in rat liver inducing coagulopathy
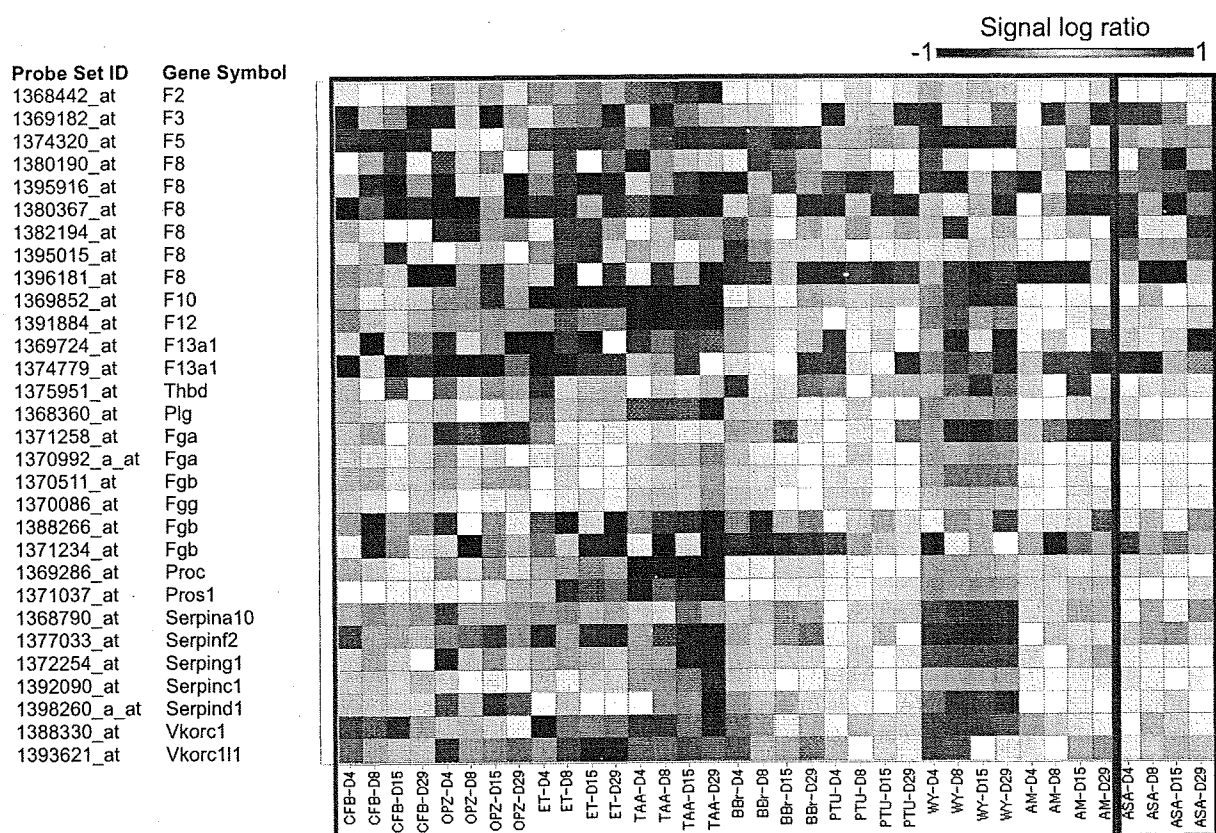
Signal log ratio

-1 ▬▬▬▬▬▬▬▬▬▬ 1

Probe Set ID	Gene Symbol
1368442_at	F2
1369182_at	F3
1374320_at	F5
1380190_at	F8
1395916_at	F8
1380367_at	F8
1382194_at	F8
1395015_at	F8
1396181_at	F8
1369852_at	F10
1391884_at	F12
1369724_at	F13a1
1374779_at	F13a1
1375951_at	Thbd
1368360_at	Plg
1371258_at	Fga
1370992_a_at	Fga
1370511_at	Fgb
1370086_at	Fgg
1388266_at	Fgb
1371234_at	Fgb
1369286_at	Proc
1371037_at	Pros1
1368790_at	Serpina10
1377033_at	Serpinf2
1372254_at	Serping1
1392090_at	Serpinc1
1398260_a_at	Serpind1
1388330_at	Vkorc1
1393621_at	Vkorc1l1

Fig. 4. Heat map of gene expression profiles of CFB, OPZ, ET, TAA, BBr, PTU, WY and AM, as well as ASA using coagulation-related 30 probe sets. Values are expressed as average log 2 ratio, for each time point at high dosage.

uting to PC1 and PC2, those with high eigenvalue, the top 20 for each, are listed in Table 4. It appears from the table that both components contain mainly lipid metabolism-related genes. PC1 also contains cellular stress-related genes such as prohibitin and CIDE-A, whereas PC2 are dominant in peroxisome-related genes, reflecting that PPARα agonists such as WY, CFB and BBr, are well separated from ET and TAA in the direction of PC2.

Verification of probe sets using ASA

To examine whether these identified probe sets have specificity to coagulopathy by liver toxicity, we applied PCA using the 344 probe sets on these 8 compounds inducing coagulopathy by liver toxicity as well as ASA, which induced prolongation of prothrombin time (Fig. 1 and Table 2), as a pharmacological effect. The results were depicted as a two-dimensional graph with PC1 (contribution rate: 38.5%) and PC2 (contribution rate: 12.4%) for each axis, where ASA did not change their position very

much on PCA, but shifted a little toward PC1 (Fig. 6). In order to visualize the difference between the compounds clearly, all the samples were aligned on a one-dimensional graph using PC1 (Fig. 7). It appeared that ASA as well as PTU showed the smallest shift among the compounds in spite of their obvious anti-coagulation effect.

DISCUSSION

Abnormality of hemostasis is often associated with hepatotoxicity. However, the precise mechanism of this acquired coagulopathy remains unclear. There are a number of proposed hypotheses regarding homeostatic disturbance in liver injury, including reduced synthesis, increased consumption, and reduced clearance of coagulation factors (Peck-Radosavljevic, 2007). In the present study, drug-induced, hepatotoxicity-related coagulopathy was able to be diagnosed by PCA using 344 genes which were commonly mobilized in 8 drugs. Although the gene
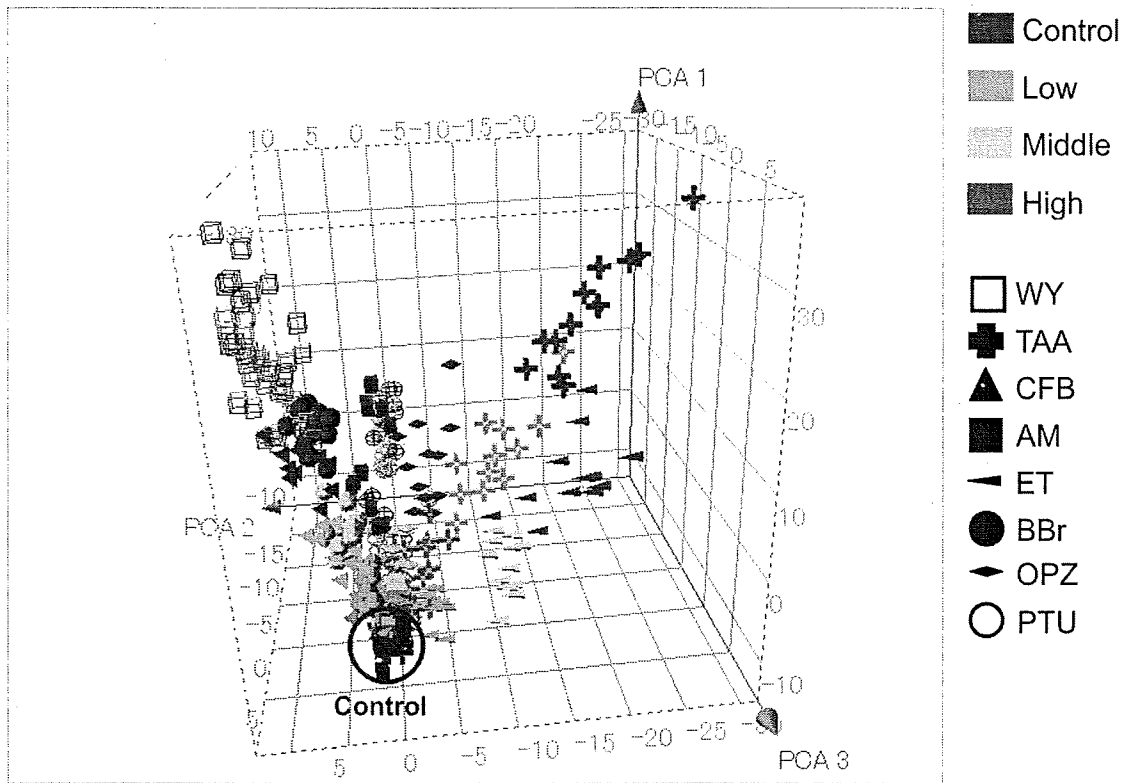
Fig. 5. Principal component analysis of gene expression profiles of CFB, OPZ, ET, TAA, BBr, PTU, WY and AM, using the commonly mobilized 344 probe sets. Results are expressed as a three dimensional graph for PC1, 2 and 3. Treated samples were dose-dependently separated from the cluster of the controls (circled by a blue line), mainly toward the direction of PC1 (contribution rate: 36.9%). For simplicity, rats receiving the same dose with different durations (3, 7, 14 and 28 days, N = 3 for each; 12 total) are expressed by the same symbol.

list contained several genes related to coagulation, those with higher contribution were mainly categorized as lipid metabolism and cell damage. PCA is a powerful tool as a non-supervised analysis, and it is quite useful to reveal the underlying mechanism when the principal components are suggestive. In the present case, however, the separation was considered attained by the indirect events in the hepatocytes that emerge as expression changes of these genes. Further analysis is obviously necessary to elucidate the mechanism of drug-induced coagulopathy by the present strategy.

As a part of the multifactorial role of liver in protein synthesis, most of the coagulation factors (fibrinogen, prothrombin, factor-V, -VII, -VIII, -IX, -X, -XI, -XII, -XIII, prekallikrein), natural anticoagulants (antithrombin-III, heparin cofactor-II, protein C, protein S, TFPI-1, TFPI-2), and components of the fibrinolytic system (plasminogen, α2-antiplasmin, TAFI) are produced in the liver (Watson,

1999; Berndt *et al.*, 2001; Savage *et al.*, 1992; Caldwell *et al.*, 2004). Pathophysiological changes in these can be detected by measurement of individual coagulation factors, or through the prolongation of PT or APTT, which are cumulatively responsive to most coagulation factors synthesized by the liver. Therefore, coagulation could be attributed to a vital synthetic capacity of the organ, not always, but at least to some extent. In the present study, a decrease in mRNA levels of some coagulation factors was observed, and it might be due to a malfunction of hepatocytes, not due to necrosis of hepatocytes, because no obvious leakage of hepatic enzymes was detected. This suggests it might be possible to detect a functional disturbance within hepatocytes by gene expression analysis. Another interesting point is that the pattern of changes in gene expression (Fig. 4) looks different among drugs, dose levels, and time points. A simple interpretation is that a decrease in coagulation factors or an increase in

Table 4. Probe sets contributing PC1 (left) and PC2 (right) in the PCA in Fig. 5. Top 20 probe sets with highest eigenvalue are listed for each component. Shaded probe sets are common in both PC1 and PC2.

|	Probe sets contributing PC1				Probe sets contributing PC2		
ranking	Probe set ID	Gene title	Eigenvalue	Ranking	Probe set ID	Gene title	Eigenvalue
1	1368317_at	aquaporin 7	0.070009144	1	1389169_at	similar to 4631434O19Rik protein	0.076072075
2	1368037_at	carbonyl reductase 1	0.068086758	2	1367672_at	peroxisomal multifunctional enzyme type II	0.075988223
3	1367926_at	prohibitin	0.067983584	3	1374475_at	similar to alpha/beta hydrolase-1	0.073630648
4	1371886_at	similar to carnitine acetyltransferase	0.067583732	4	1380431_at	similar to KIAA0564 protein	0.072382202
5	1367937_at	aldehyde reductase like 6	0.067191284	5	1388531_at	similar to 4631434O19Rik protein	0.071730013
6	1390358_at	calcium channel, voltage dependent, alpha2/delta subunit 3	0.066297774	6	1367763_at	acetyl-coenzyme A acetyltransferase 1	0.06845887
7	1368206_at	4,8-dimethylnonanoyl-CoA thioesterase	0.066110077	7	1369050_at	phosphatidylinositol 3-kinase, C2 domain containing, gamma polypeptide	0.066532737
8	1371985_a_at	HLA-B associated transcript 5	0.065669124	8	1387100_at	aquaporin 3	0.065969965
9	1367767_at	3-hydroxy-3-methylglutaryl CoA lyase	0.065441346	9	1367897_at	acyl-Coenzyme A dehydrogenase, very long chain	0.065740005
10	1398249_at	solute carrier family 25 member 20	0.064983662	10	1367777_at	2,4-dienoyl CoA reductase 1, mitochondrial	0.065545622
11	1388908_at	similar to Peci protein	0.064839999	11	1370818_at	2-4-dienoyl-Coenzyme A reductase 2, peroxisomal	0.065292746
12	1370491_a_at	histidine decarboxylase	0.064505345	12	1386885_at	enoyl coenzyme A hydratase 1	0.064882077
13	1375845_at	similar to 1500031O19Rik protein	0.064282403	13	1375845_at	similar to 1500031O19Rik protein	0.064743473
14	1387100_at	aquaporin 3	0.064133715	14	1368150_at	solute carrier family 27 (fatty acid transporter), member 32	0.063597102
15	1389179_at	similar to cell death activator CIDE-A	0.06405368	15	1376296_at	acyl-coA oxidase	0.063222767
16	1368977_a_at	fractured callus expressed transcript 1	0.063993326	16	1367680_at	fatty acid desaturase 2	0.062867058
17	1387740_at	peroxisomal membrane protein Pmp26p (Peroxin-11)	0.063938006	17	1368453_at	carbonyl reductase	0.062473231
18	1367927_at	prohibitin	0.063680305	18	1370814_at	cytosolic acyl-CoA thioesterase 1	0.062293648
19	1374210_at	similar to RIKEN cDNA 2510027N19	0.063409988	19	1388211_s_at	peroxisomal membrane protein Pmp26p (Peroxin-11)	0.061676191
20	1370164_at	hydroxyacyl-Coenzyme A dehydrogenase, alpha subunit	0.063337769	20	1379361_at	enoyl-Coenzyme A, hydratase	0.061650054

M. Hirode *et al.*
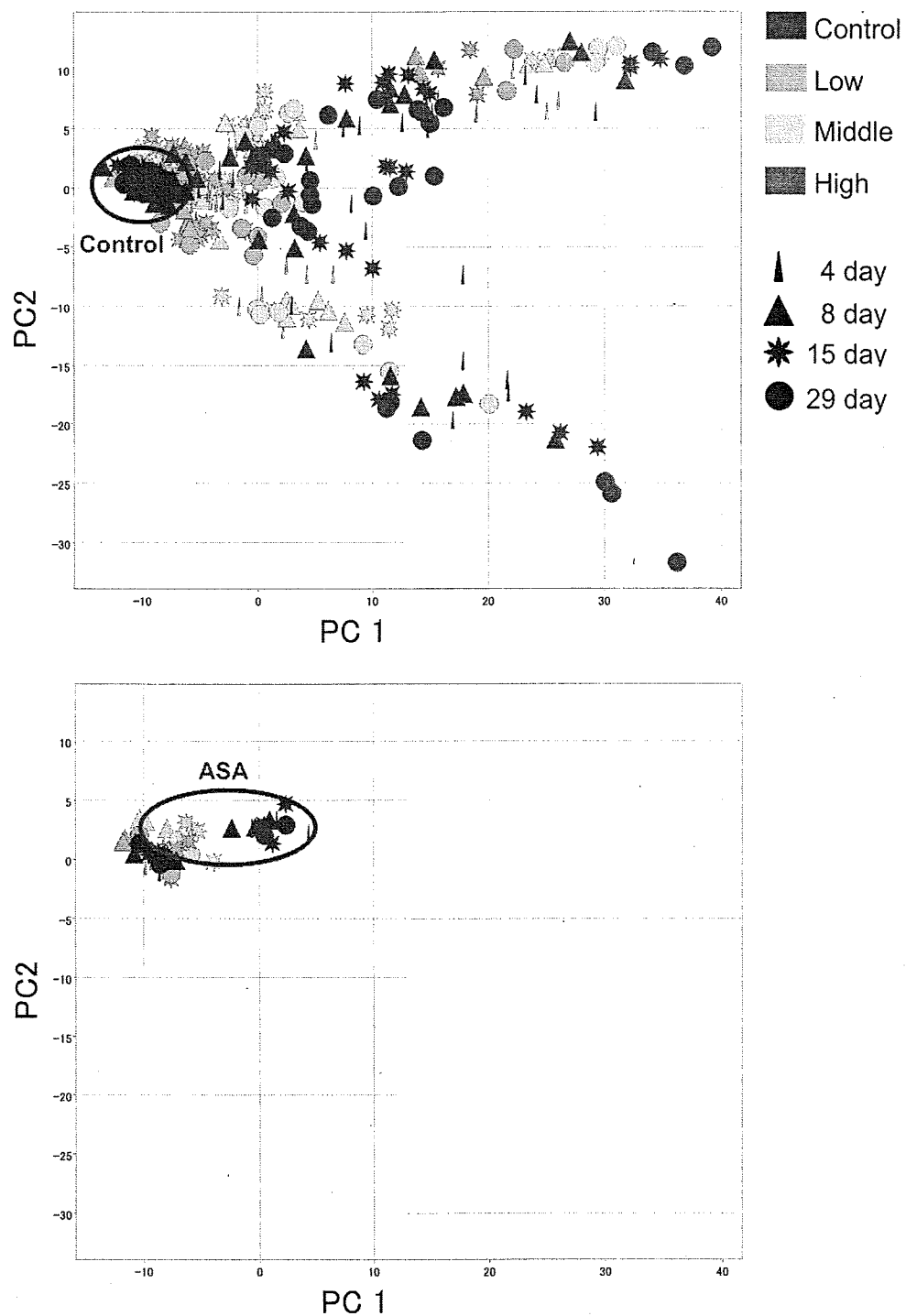
Fig. 6. Principal component analysis of gene expression profiles of 8 coagulopathic compounds with ASA. Results are expressed as a two dimensional graph for PC1 and 2. For simplicity, only dose and time are expressed by different symbols and each drug is not distinguished. In order to highlight the small separation of ASA, drugs other than ASA are eliminated from the graph and depicted in the lower panel.
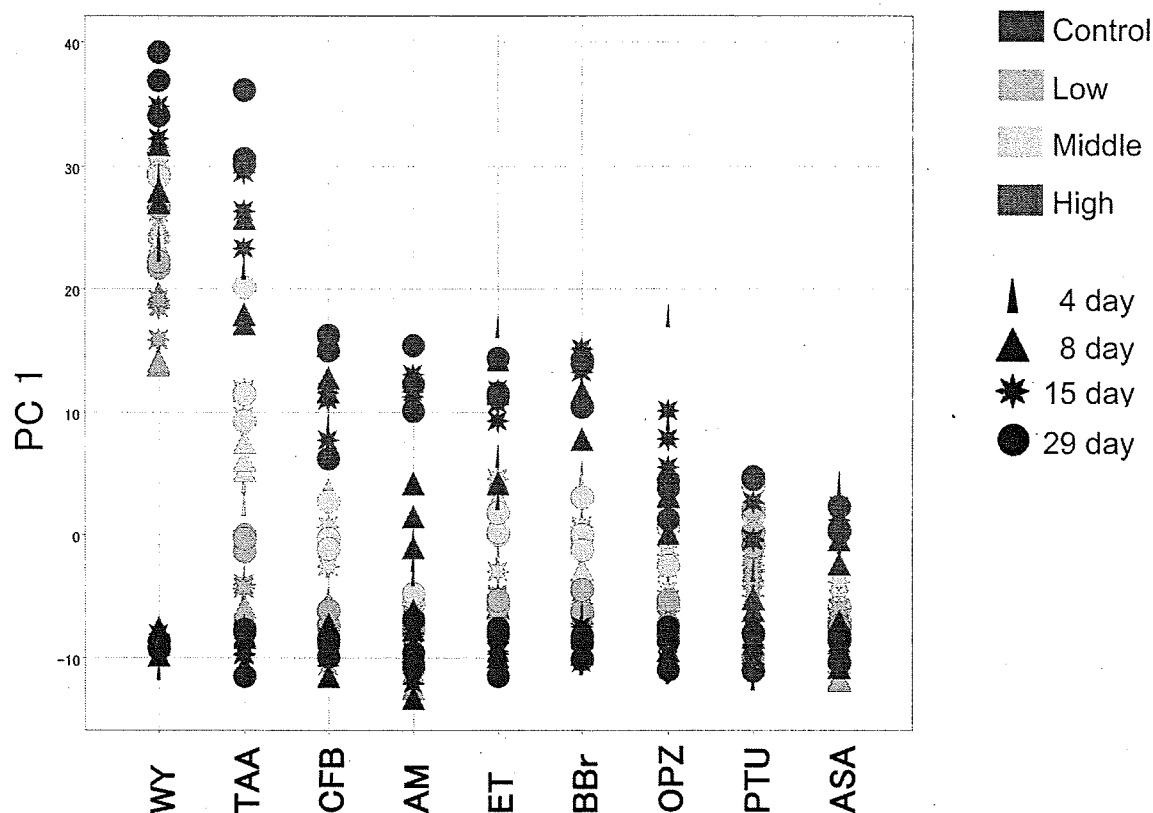
Fig. 7. Principal component analysis of gene expression profiles of 8 coagulopathic compounds with ASA. Results are expressed as a one dimensional graph with PC1 (contribution rate: 38.5%). For each drug, each individual rat is depicted by a symbol with a different color and shape, as shown on the right panel. Note that ASA and PTU show low PC1 values.

anti-coagulation factors leads to prolongation. When the opposite phenomena were observed, they could be a feedback mechanism to maintain homeostasis. This might enable us to analyze the underlying toxicological mechanism of coagulopathy or hepatic dysfunction.

Vitamin K is an essential co-factor for biosynthesis of factors II, VII, IX and X, as well as proteins C, S and Z, as it catalyzes γ-carboxylation of glutamic acid in their amino-terminal region (Vacca, 2000). Blood coagulation time is prolonged in vitamin K deficiency or warfarin therapy. In the consequence of severe vitamin K deficiency, it was reported that decarboxylated precursors, named precursors induced by vitamin K absence (PIVKA), were produced causing coagulopathy because of their diminished activity (Amitrano *et al.*, 2002). It is possible that the reduction of coagulation factors in plasma observed in the present study was due to vitamin K-related events. Vkorc1, which synthesizes vitamin K from vitamin K epoxide, has been identified as a target of warfarin, and

its genetic variation explains the variability of the effective warfarin dose among individuals (Wadelius *et al.*, 2007). In the present study, typical coagulopathy-inducing drugs generally inhibit the expression of Vkorc1, and this was consistent with their reduced coagulation. Interestingly, however, its paralogous gene, Vkorc1l1, was up-regulated in most cases (Fig. 4). Vkorc1l1 was proved not to be involved in the variability of warfarin dose requirement and its physiological function is totally unknown (Yin *et al.*, 2008). It is of interest that the directions of expression changes in these two paralogous genes were opposed. Further investigation is necessary to elucidate the role of their products in the pathogenesis of drug-induced coagulopathy.

α1-Antitrypsin (AAT; SERPIN A1) is a serpin in plasma (Silverman *et al.*, 2001; Kalsheker *et al.*, 2002). AAT has a broad range of activities, including inhibition of the serine proteinases. Increase of serpins might also be related to prolongation of coagulation time, since

Kazal type serine protease inhibitors have been suggested as candidates for thrombin inhibition (van de Locht *et al.*, 1995; Gettins, 2002). In the present study, the expression of serpines were mostly reduced, namely, opposite to what is expected from coagulation. This could be interpreted as a feedback mechanism against prolonged coagulation. Some cytokines, such as interleukin-6 (IL-6), have the largest stimulatory effect on production of hepatocyte derived AAT. Interferon C and transforming growth factor β also modulate the hepatocyte response to IL-6 (Mackiewicz and Kushner, 1990; Magielska-Zero *et al.*, 1988). As IL-6 and TNF-α were also both markedly increased in acute liver injury (Kerr, 2003), the interpretation of the results of serpins are quite complex and difficult.

In the present study, fibrates, such as WY and CFB, and BBr, which has PPARα agonistic activity (Tamura *et al.*, 2006), were separated from their controls by PCA. It is reported that PPARα agonists down-regulated human fibrinogen-β via negative interference with C/EBPβ as a result of titration of GRIP1/TIF2 (Gervois *et al.*, 2001). This explains the present observation that PPARα agonists decreased plasma fibrinogen, whereas a question remains why BBr did not reduce the fibrinogen level.

Using PC1 as an indicator of coagulopathy, PTU and ASA were the lowest among the compounds. It is well known that ASA at its clinical dose elicits a selective antiplatelet activity without affecting blood coagulation by the route of inactivating cyclooxygenase-1 via irreversible acetylation and subsequent reduction of thromboxane A2 (Selwyn, 2003). In the overdose range, especially in animal toxicity studies, ASA may induce prolongation of PT, attributed not to ASA itself, but to its metabolite, salicylate (Cattaneo *et al.*, 1983). Sustained elevation of serum salicylate causes reduction of vitamin K-dependent coagulation factors II, VII and X, by inhibiting vitamin K quinone reductase (Yip, 2004). As for PTU, it is also known to inhibit the vitamin K dependent step in clotting factor synthesis (Lipsky and Gallego, 1988). In fact, blood coagulation-related genes among selected genes showed quite weak changes by both drugs. Albeit the same phenotype was observed, we could still distinguish ASA and PTU, which directly affected synthesis of coagulation factors, from other drugs that caused coagulation abnormality due to hepatic failure.

In conclusion, the genes extracted in the present study could be a useful source for developing biomarkers for hepatotoxicant-induced coagulation abnormality. Although further refinement and tuning of the present strategy is obviously needed, it is a good candidate for a starting point that could lead to mechanism-based diagnosis or prediction of coagulopahy in toxicity tests in the early stage of drug development.

ACKNOWLEDGMENTS

REFERENCES

Amitrano, L., Guardascione, M.A., Brancaccio, V. and Balzano, A. (2002): Coagulation disorders in liver disease. Semin. Liver Dis., **22**, 83-96.

Berndt, M.C., Shen, Y., Dopheide, S.M., Gardiner, E.E. and Andrews, R.K. (2001): The vascular biology of the glycoprotein Ib-IX-V complex. Thromb. Haemost., **86**, 178-188.

Caldwell, S.H., Chang, C. and Macik, B.G. (2004): Recombinant activated factor VII (rFVIIa) as a hemostatic agent in liver disease: a break from convention in need of controlled trials. Hepatology, **39**, 592-598.

Cattaneo, M., Chahil, A., Somers, D., Kinlough-Rathbone, R.L., Packham, M.A. and Mustard, J.F. (1983): Effect of aspirin and sodium salicylate on thrombosis, fibrinolysis, prothrombin time, and platelet survival in rabbits with indwelling aortic catheters. Blood, **61**, 353-361.

Dennis, G.Jr., Sherman, B.T., Hosack, D.A., Yang, J., Gao, W., Lane, H.C. and Lempicki, R.A. (2003): DAVID: Database for Annotation, Visualization, and Integrated Discovery. Genome Biol., **4**, P3.

Fujii, T. (1997): Toxicological correlation between changes in blood biochemical parameters and liver histopathological findings. J. Toxicol. Sci., **22**, 161-183.

Gervois, P., Vu-Dac, N., Kleemann, R., Kockx, M., Dubois, G., Laine, B., Kosykh, V., Fruchart, J.C., Kooistra, T. and Staels, B. (2001): Negative regulation of human fibrinogen gene expression by peroxisome proliferator-activated receptor alpha agonists via inhibition of CCAAT box/enhancer-binding protein beta. J. Biol. Chem., **276**, 33471-33477.

Gettins, P.G. (2002): Serpin structure, mechanism, and function. Chem. Rev., **102**, 4751-4804.

Hirode, M., Ono, A., Miyagishima, T., Nagao, T., Ohno, Y. and Urushidani, T. (2008): Gene expression profiling in rat liver treated with compounds inducing phospholipidosis. Toxicol. Appl. Pharmacol., **229**, 290-299.

Hirode, M., Horinouchi, A., Uehara, T., Ono, A., Miyagishima, T., Yamada, H., Nagao, T., Ohno, Y. and Urushidani, T. (2009): Gene expression profiling in rat liver treated with compounds inducing elevation of bilirubin. Hum. Exp. Toxicol. (in press).

Kalsheker, N., Morley, S. and Morgan, K. (2002): Gene regulation of the serine proteinase inhibitors alpha1-antitrypsin and alpha1-antichymotrypsin. Biochem. Soc. Trans., **30**, 93-98.

Kerr, R. (2003): New insights into haemostasis in liver failure. Blood. Coagul. Fibrinolysis, **14 Suppl 1**, S43-45.

Kerr, R., Newsome, P., Germain, L., Thomson, E., Dawson, P., Stirling, D. and Ludlam, C.A. (2003): Effects of acute liver injury on blood coagulation. J. Thromb. Haemost., **1**, 754-759.

Kiyosawa, N., Uehara, T., Gao, W., Omura, K., Hirode, M., Shimizu, T., Mizukawa, Y., Ono, A., Miyagishima, T., Nagao, T. and

Urushidani, T. (2007): Identification of glutathione depletion-responsive genes using phorone-treated rat liver. J. Toxicol. Sci., 32, 469-486.

Lipsky, J.J. and Gallego, M.O. (1988): Mechanism of thioamide antithyroid drug associated hypoprothrombinemia. Drug. Metabol. Drug. Interact., 6, 317-326.

Mackiewicz, A. and Kushner, I. (1990): Transforming growth factor beta 1 influences glycosylation of alpha 1-protease inhibitor in human hepatoma cell lines. Inflammation., 14, 485-497.

Magielska-Zero, D., Bereta, J., Czuba-Pelech, B., Pajdak, W., Gauldie, J. and Koj, A. (1988): Inhibitory effect of human recombinant interferon gamma on synthesis of acute phase proteins in human hepatoma Hep G2 cells stimulated by leukocyte cytokines, TNF alpha and IFN-beta 2/BSF-2/IL-6. Biochem. Int., 17, 17-23.

Omura, K., Kiyosawa, N., Uehara, T., Hirode, M., Shimizu, T., Miyagishima, T., Ono, A., Nagao, T. and Urushidani,.T. (2007): Gene expression profiling of rat liver treated with serum triglyceride-decreasing compounds. J. Toxicol. Sci., 32, 387-399.

Ozer, J., Ratner, M., Shaw, M., Bailey, W. and Schomaker, S. (2008): The current state of serum biomarkers of hepatotoxicity. Toxicology., 245, 194-205.

Peck-Radosavljevic, M. (2007): Review article: coagulation disorders in chronic liver disease. Aliment. Pharmacol. Ther., 26 Suppl 1, 21-28.

Savage, B., Shattil, S.J. and Ruggeri, Z.M. (1992): Modulation of platelet function through adhesion receptors. a dual role for glycoprotein IIb-IIIa (integrin alpha IIb beta 3) mediated by fibrinogen and glycoprotein Ib-von Willebrand factor. J. Biol. Chem., 267, 11300-11306.

Selwyn, A.P. (2003): Prothrombotic and antithrombotic pathways in acute coronary syndromes. Am. J. Cardiol., 91, 3H-11H.

Silverman, G.A., Bird, P.I., Carrell, R.W., Church, F.C., Coughlin, P.B., Gettins, P.G., Irving, J.A., Lomas, D.A., Luke, C.J., Moyer, R.W., Pemberton, P.A., Remold-O'Donnell, E., Salvesen, G.S., Travis, J. and Whisstock, J.C. (2001): The serpins are an expanding superfamily of structurally similar but functionally diverse proteins. Evolution, mechanism of inhibition, novel functions, and a revised nomenclature. J. Biol. Chem., 276, 33293-33296.

Takashima, K., Mizukawa, Y., Morishita, K., Okuyama, M.,

Kasahara, T., Toritsuka, N., Miyagishima, T., Nagao, T. and Urushidani, T. (2006): Effect of the difference in vehicles on gene expression in the rat liver--analysis of the control data in the Toxicogenomics Project Database. Life Sci., 78, 2787-2796.

Tamura, K., Ono, A., Miyagishima, T., Nagao, T. and Urushidani, T. (2006): Profiling of gene expression in rat liver and rat primary cultured hepatocytes treated with peroxisome proliferators. J. Toxicol. Sci., 31, 471-490.

Uehara, T., Hirode, M., Ono, A., Kiyosawa, N., Omura, K., Shimizu, T., Mizukawa, Y., Miyagishima, T., Nagao, T. and Urushidani, T. (2008): A toxicogenomics approach for early assessment of potential non-genotoxic hepatocarcinogenicity of chemicals in rats. Toxicology., 250, 15-26.

Urushidani, T. (2008): Prediction of Hepatotoxicity Based on the Toxicogenomics Database. In Hepatotoxicity: from Genomics to in vitro and in vivo Models. (Sahu, S.C. ed.), pp. 507-529, John Wiley & Sons, Chichester, West Sussex, England.

Vacca, J.P. (2000): New advances in the discovery of thrombin and factor Xa inhibitors. Curr. Opin. Chem. Biol., 4, 394-400.

van de Locht, A., Lamba, D., Bauer, M., Huber, R., Friedrich, T., Kröger, B., Höffken, W. and Bode, W. (1995): Two heads are better than one: crystal structure of the insect derived double domain Kazal inhibitor rhodniin in complex with thrombin. EMBO J., 14, 5149-5157.

Wadelius, M., Chen, L.Y., Eriksson, N., Bumpstead, S., Ghori, J., Wadelius, C., Bentley, D., McGinnis, R. and Deloukas, P. (2007): Association of warfarin dose with genes involved in its action and metabolism. Hum. Genet., 121, 23-34.

Watson, S.P. (1999): Collagen receptor signaling in platelets and megakaryocytes. Thromb. Haemost., 82, 365-376.

Yin, T., Hanada, H., Miyashita, K., Kokubo, Y., Akaiwa, Y., Otsubo, R., Nagatsuka, K., Otsuki, T., Okayama, A., Minematsu K., Naritomi, H., Tomoike, H. and Miyata, T. (2008): No association between vitamin K epoxide reductase complex subunit 1-like 1 (VKORC1L1) and the variability of warfarin dose requirement in a Japanese patient population. Thromb. Res., 122, 179-184.

Yip, L. (2004): Salicylates. In Medical Toxicology (Dart, R.C. et al., ed.), pp. 739-749, Lippincott Williams & Wilkins, Philadelphia, PA, USA.
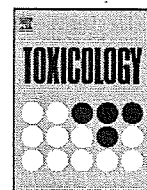
Identification of genomic biomarkers for concurrent diagnosis of drug-induced renal tubular injury using a large-scale toxicogenomics database

Chiaki Kondo [a,1], Yohsuke Minowa [b,*,1], Takeki Uehara [a,**,1], Yasushi Okuno [c], Noriyuki Nakatsu [b], Atsushi Ono [d], Toshiyuki Maruyama [a], Ikuo Kato [a], Jyoji Yamate [e], Hiroshi Yamada [b], Yasuo Ohno [f], Tetsuro Urushidani [b,g]

[a] Developmental Research Laboratories, Shionogi & Co., Ltd., 3-1-1, Futaba-cho, Toyonaka, Osaka, Japan
[b] Toxicogenomics-Informatics Project, National Institute of Biomedical Innovation, 7-6-8 Asagi, Ibaraki, Osaka 567-0085, Japan
[c] Department of Systems Bioscience for Drug Discovery, Graduate School of Pharmaceutical Sciences, Kyoto University, 46-29, Yoshida Shimoadachi-cho, Kyoto 606-8501, Japan
[d] Division of Risk Assessment, National Institute of Health Sciences, Kamiyoga 1-18-1, Setagaya-ku, Tokyo 158-8501, Japan
[e] Department of Veterinary Pathology, Graduate School of Agriculture and Biological Science, Osaka Prefecture University, 1-1 Gakuen- cho, Sakai, Osaka 599-8531, Japan
[f] National Institute of Health Sciences, Kamiyoga 1-18-1, Setagaya-ku, Tokyo 158-8501, Japan
[g] Department of Pathophysiology, Faculty of Pharmaceutical Sciences, Doshisha Women's College of Liberal Arts, Kodo, Kyotanabe, Kyoto 610-0395, Japan

ARTICLE INFO

ABSTRACT

Drug-induced renal tubular injury is one of the major concerns in preclinical safety evaluations. Toxicogenomics is becoming a generally accepted approach for identifying chemicals with potential safety problems. In the present study, we analyzed 33 nephrotoxicants and 8 non-nephrotoxic hepatotoxicants to elucidate time- and dose-dependent global gene expression changes associated with proximal tubular toxicity. The compounds were administered orally or intravenously once daily to male Sprague-Dawley rats. The animals were exposed to four different doses of the compounds, and kidney tissues were collected on days 4, 8, 15, and 29. Gene expression profiles were generated from kidney RNA by using Affymetrix GeneChips and analyzed in conjunction with the histopathological changes. We used the filter-type gene selection algorithm based on t-statistics conjugated with the SVM classifier, and achieved a sensitivity of 90% with a selectivity of 90%. Then, 92 genes were extracted as the genomic biomarker candidates that were used to construct the classifier. The gene list contains well-known biomarkers, such as *Kidney injury molecule 1, Ceruloplasmin, Clusterin, Tissue inhibitor of metallopeptidase 1*, and also novel biomarker candidates. Most of the genes involved in tissue remodeling, the immune/inflammatory response, cell adhesion/proliferation/migration, and metabolism were predominantly up-regulated. Down-regulated genes participated in cell adhesion/proliferation/migration, membrane transport, and signal transduction. Our classifier has better prediction accuracy than any of the well-known biomarkers. Therefore, the toxicogenomics approach would be useful for concurrent diagnosis of renal tubular injury.

© 2009 Elsevier Ireland Ltd. All rights reserved.

1. Introduction

Toxicogenomics, which is the application of microarray technologies to toxicology, is becoming a generally accepted approach for identifying chemicals with potential safety problems. Identifying drug safety liabilities or predictive biomarkers for drug-induced organ damage at or before the preclinical stages of drug development is of great importance to pharmaceutical companies. The ability to determine whether or not to pursue the development of a drug based on safety would greatly reduce the cost of drug development and improve the attrition rate of new chemical entities. Currently, preclinical drug safety evaluation relies mainly on complex histopathological or clinical pathological analysis. These traditional approaches have proven to be highly successful but may fail to detect prodromal and early stages of toxicity. Genomic data can be more sensitive and objective than traditional methods for the early prediction of compound-induced toxicity. Microarray expression profiling during preclinical drug development is expected to aid in uncovering unexpected or secondary pharmacology, predicting adverse effects, and understanding the mechanisms of drug action or toxicity (Battershill,

2005; Heinloth et al., 2004; Irwin et al., 2004; Searfoss et al., 2005).

The kidney is a major organ for the filtration, secretion, re-absorption and ultimately the excretion of drugs or drug metabolites. Nephrotoxicity frequently occurs after administration of various drugs or xenobiotics. The tubular cells of the kidney are particularly vulnerable to drug-induced injury, and thus renal tubular toxicity is a major concern in preclinical safety evaluations. Drug-induced tubular damage has been well documented and extensively studied (Perazella, 2005). The prediction and diagnosis of preclinical renal tubular toxicity based on molecular methods that use microarray gene expression data have been attempted. Fielden et al. (2005) assessed predicative gene expression endpoints at early time points proceeding the onset of any signs of renal tubular pathology, and they achieved a prediction accuracy of 76%. In a separate study that assessed the expression profiling endpoints in parallel with the histopathological diagnosis of concurrent renal tubular toxicity, the performance was improved and a sensitivity of 82% was achieved with 100% of selectivity (Thukral et al., 2005). Furthermore, Jiang et al. (2007) achieved a sensitivity of 88% and a specificity of 91% using the expression profiling endpoints in parallel with the histopathological diagnosis of concurrent renal tubular toxicity. It is thought that concurrent diagnosis is easier than the prediction of future onset because the early stage toxic gene expression changes are heterogenic between different compounds, but the gene expression changes concurrent with the same toxic endpoints are comparatively homogenous among different compounds.

The Toxicogenomics Project (TGP) is a public–private collaborative project of the National Institute of Health Sciences, the National Institute of Biomedical Innovation, and 15 pharmaceutical companies in Japan that began in 2002 (Urushidani and Nagao, 2005). Its aim is to construct a large-scale toxicology database of transcriptomes that are useful to predict the toxicity of new chemical entities in the early stages of drug development. Until now, about 150 chemicals, primarily medicinal compounds, were selected and gene expression profiles of multiple doses and times in the rat liver and kidney, and rat and human hepatocytes were comprehensively analyzed by using the Affymetrix GeneChip® (over 27,000 profiles). These gene expression profiles, conjugated with the histopathological changes, the results of blood biochemical examinations, and the other phenotypic profiles, are stored in our database with a web-based tool for statistical analysis named TG-GATEs (Genomics Assisted Toxicity Evaluation System developed by Toxicogenomics Project in Japan). Thirteen of the 150 chemicals were typical nephrotoxicants or drugs showing clinical side effects (e.g., cisplatin, carboplatin, gentamicin, vancomycin, phenacetin, and bucetin), and 20 chemicals exhibited nephrotoxicity in addition to hepatotoxicity (e.g., phenylbutazone, ethionine, and indomethacin). We measured gene expression profiles in the kidney after exposure to the group of 33 nephrotoxicants and a negative control group of 8 hepatotoxicants; thus, data from 41 chemicals are presently available for the analysis of nephrotoxicity. The specific aim of the present study was to develop identifiers for concurrent diagnosis of drug-induced tubular injury based on gene expression profiles available from our toxicogenomics database.

The possibility that a genomics evaluation could lead to the elucidation of biomarkers that provide additional sensitivity and/or earlier detection of renal tubular damage is intriguing. A biomarker discovery effort requires experimental designs that encompass several compounds of diverse chemical natures that cause the same toxic endpoint. In addition, multiple time points and doses are necessary to tease out the gene expression changes that are early indicators of the severity and progression of lesions. Therefore, it is reasonable to at first elucidate genetic biomarkers for concur-

rent diagnosis at the same toxic endpoints, because these gene expression profiles are relatively homogenous compared to the profiles at the early stage of toxicity. Moreover, in the examination of sensitive toxicogenomics data, it is necessary to distinguish adverse changes from changes that are normal physiologic adaptive responses within a no observable adverse effect level (NOAEL). Also, when a biomarker is intended for broad research or regulatory use, the size and diversity of the training set must be considered, and validation of the biomarker on external data must be demonstrated (Somorjai et al., 2003; Ransohoff, 2004). A large-scale toxicogenomics database containing data from multiple time points and drug doses is useful to reliably assess hypotheses generated in other studies that have used comparatively small datasets.

In the present analysis, we extracted candidate biomarkers for the concurrent diagnosis of nephrotoxicity using the large-scale microarray dataset generated in our project. The microarray samples treated with nephrotoxicants and hepatotoxicants were divided into positives and negatives of the training set according to their histopathological findings, to perform supervised classification algorithms after selecting differentially expressed genes. We used three different types of algorithms for gene selection and classification to select the most appropriate method for our dataset and the development of statistically robust analysis. The external test sets were randomly generated 100 times by dividing the training set into subsets, and the prediction accuracy was calculated by summarizing the prediction results of the external test sets. As a result, we achieved a sensitivity of 90% with a selectivity of 90%. Then, 92 genes were extracted as the genomic biomarker candidates that were used to construct the classifier. The group of extracted genes contains well-known biomarkers, such as *Kidney injury molecule-1* (*Kim1*), *Ceruloplasmin* (*Cp*), *Clusterin* (*Clu*), *Tissue inhibitor of metallopeptidase 1* (*Timp1*), *Secreted phosphoprotein 1* (*Spp1*), and also novel biomarker candidates. Our multigene-based classifier had better classification accuracy than any of the single well-known biomarkers; therefore, toxicogenomics would be more useful for concurrent diagnosis of renal tubular injury than any of the previous criteria.

2. Materials and methods

2.1. Compounds

The chemical name, abbreviation, dosage, administration route and vehicle for each compound used in this study are summarized in Table 1.

2.2. Animal treatment

Five-week-old male Sprague-Dawley rats were obtained from Charles River Japan, Inc. (Kanagawa, Japan). After a 7-day quarantine and acclimatization period, 6-week-old animals were assigned to dosage groups (five rats per group) using a computerized stratified random grouping method based on individual body weight. The animals were individually housed in stainless-steel cages in an animal room that was lighted for 12 h (7:00–19:00) each day, ventilated with an air-exchange rate of 15 times per hour, and maintained at 21–25 °C with a relative humidity of 40–70%. Each animal was allowed free access to water and pellet diet (CRF-1, sterilized by radiation, Oriental Yeast Co., Ltd., Tokyo, Japan). Rats in each group received orally administered drugs that were suspended or dissolved in 0.5% methylcellulose solution (MC) or corn oil according to their dispersibility, with the exceptions of cisplatin, carboplatin, 2-bromoethylamine, cephalothin, puromycin aminonucleoside, gentamicin, vancomycin and doxorubicin, which were dissolved in saline and administered intravenously. The animals were treated for 3, 7, 14, or 28 days and sacrificed 24 h after the last dose. Blood samples from the abdominal aorta were collected in a heparinized tube after the rats were anesthetized with ether. After collecting the blood, the animals were euthanized by exsanguination from the abdominal aorta. For histopathological examination, kidney samples were fixed in 10% neutral-buffered formalin, dehydrated in alcohol and embedded in paraffin. Paraffin sections were prepared and stained using standard methods for hematoxylin and eosin staining (H&E). The experimental protocols were reviewed and approved by the Ethics Review Committee for Animal Experimentation of the National Institute of Health Sciences.

Table 1

In vivo compound treatments used in training and testing.

Compound	Dose (mg/kg/day; repeated)	Vehicle	Route
Gentamicin sulphate	~100	Saline	iv
Vancomycin hydrochloride	~200	Saline	iv
2-Bromoethylamine hydrobromide	~20	Saline	iv
Phenylbutazone	~200	0.5% MC	po
Cyclosporine A	~100	Corn oil	po
Thioacetamide	~45	0.5% MC	po
K17	~600	0.5% MC	po
Triamterene	~150	0.5% MC	po
Allopurinol	~150	0.5% MC	po
Nitrofurantoin	~100	0.5% MC	po
Ethionine	~250	0.5% MC	po
N-Phenylanthranilic acid	~1000	0.5% MC	po
Cisplatin	~1	Saline	iv
Phenacetin	~1000	0.5% MC	po
Puromycin aminonucleoside	~40	Saline	iv
Lomustine	~6	0.5% MC	po
Cyclophosphamide	~15	0.5% MC	po
Carboplatin	~10	Saline	iv
Hexachlorobenzene	~300	Corn oil	po
Captopril	~1000	0.5% MC	po
Enalapril	~600	0.5% MC	po
Indomethacin	~5	0.5% MC	po
Doxorubicin hydrochloride	~1	Saline	iv
Ethinyl estradiol	~10	Corn oil	po
Monocrotaline	~30	0.5% MC	po
Acetaminophen	~1000	0.5% MC	po
Cephalothin sodium	~2000	Saline	iv
Bucetin	~1000	0.5% MC	po
Methyltestosterone	~300	0.5% MC	po
Rifampicin	~200	0.5% MC	po
Imipramine hydrochloride	~100	0.5% MC	po
Acetazolamide	~600	0.5% MC	po
Caffeine	~100	0.5% MC	po
Valproic acid	~450	0.5% MC	po
Clofibrate	~300	Corn oil	po
Allyl alcohol	~45	Corn oil	po
Omeprazole	~1000	0.5% MC	po
Bromobenzene	~300	Corn oil	po
Ketoconazole	~100	0.5% MC	po
Ciprofloxacin	~1000	0.5% MC	po
Erythromycin ethylsuccinate	~1000	0.5% MC	po

Male SD rats received oral or intravenous doses once daily (6 weeks of age, $n = 5$). Four, 8, 15, and 29 days after the start of repeated administrations, the kidney tissues were collected and used for gene expression analysis (Affymetrix GeneChip®, $n = 3/5$). Four doses were used for each compound including vehicle control (vehicle control, low, middle, high dose level). Different doses were used for single and repeated administration. po: peroral, iv: intravenous.

2.3. Microarray analysis

An aliquot of the tissue sample (whole slice; about 30 mg) for RNA analysis was obtained from the kidney in each animal immediately after sacrifice. Tissue samples were kept in RNAlater® (Ambion, Austin, TX, USA) overnight at 4 °C, and then frozen at −80 °C until use. Kidney samples were homogenized with buffer RLT that was supplied with the RNeasy mini kit (Qiagen, Valencia, CA, USA), and total RNA was isolated according to the manufacturer's instructions. Microarray analysis was conducted on 3 of 5 samples for each group by using GeneChip® Rat Genome 230 2.0 Arrays (Affymetrix, Santa Clara, CA, USA), which contain 31,042 probe sets. The procedure was conducted basically according to the manufacturer's instructions by using One-Cycle Target Labeling and Control Reagents (Affymetrix) for cDNA synthesis, purification, and the synthesis of biotin-labeled cRNA. Ten micrograms of fragmented cRNA was hybridized to a Rat Genome 230 2.0 Array for 18 h at 45 °C at 60 rpm, after which the array was washed and stained with streptavidin-phycoerythrin by using Fluidics Station 400 (Affymetrix) and then scanned with a Gene Array Scanner (Affymetrix). The digital image files were preprocessed by Affymetrix Microarray Suite version 5.0 (MAS5.0) and converted into base10 logarithmic values. Then, these values were normalized into Z-scores by using Tukey's biweight algorithm. The normalized datasets were reversed into non-logarithmic values by calculating their exponential numbers in decimal, and the log-ratio of base 2 to the means of the control groups were calculated.

2.4. Gene selection and supervised classification

High-dose groups of 23 compounds that caused necrosis, degeneration, or regeneration in the renal tubules during chronic exposure were defined as the positive set. Low-dose groups of all of 41 compounds and high-dose groups of the eight hepatotoxicants, which had no histopathological findings, were defined as the neg-

ative set. Other high-dose groups of 10 compounds and middle-dose groups were treated as the external test set. Both filter-type and wrapper-type gene selection algorithms and Support Vector Machine (SVM; Vapkin, 1995) and Prediction Analysis of Microarrays (PAM; Tibshirani et al., 2002) supervised classification algorithms were used to extract the biomarker candidates and construct classifiers using the selected genes. Recursive feature elimination (SVM-RFE; multivariate type; Guyon et al., 2002) and nearest shrunken centroid (PAM; univariate type) were used as wrapper-type gene selection algorithms, and Intensity-Based Moderated T-statistics (IBMT; Sartor et al., 2006) was used as a filter-type gene selection algorithm (SVM was used as the classifier, in this case).

Five-fold cross-validation (CV) was executed for optimization of the classifiers and to calculate their prediction accuracies. At first, the whole positive and negative training datasets were randomly divided into five subsets of roughly equal size. The SVM and PAM were trained with a selection of optimal genes on eight subsets (four positive subsets and four negative subsets) and then applied to the remaining subset as the test dataset. The negative samples of the test subset were randomly excluded to adjust the number to the positive samples before prediction. Before training of the SVM, optimal genes were selected from the training set by using "Recursive Feature Elimination" (SVM-RFE) or "Intensity-Based Moderated T-statistics" (SVM+IBMT). One to 99 of the top-ranked genes of each selection strategy were used to construct the classifiers. Also, in the case of the PAM classifier, 3 to 10 were used as the threshold of the centroid shrinkage to select top-ranked genes. The feature genes used in each training set were filtered by MAS5.0 P/A-call (excluded the probes that were judged as absent in all samples of the training set) and fold change (excluded the probes whose absolute $\log_2$ ratio values were less than 1 between the positives and the negatives) during the 5-fold CV, before being selected and ranked by the feature selection algorithms.

The classifiers were also tested by making the external test datasets by randomly dividing 23 compounds containing positive samples and 18 compounds containing

only negative samples into 5 subsets. An arbitrary subset (combining a positive subset and a negative subset) and the remaining subsets were respectively treated as the external test set and the training set. Compounds of the test subset containing only negative samples were randomly excluded to adjust the number of negative samples to the positive samples before prediction. The feature genes were selected from the training set and used to construct the classifier, which was used to predict the external test set. This process was repeated 100 times, and the prediction accuracy was calculated as the sum of all of the prediction results calculated. Then, the whole positive and negative datasets were used to construct the classifier and to predict the external test set (high-dose groups of 10 compounds and middle-dose groups of all of 41 compounds).

3. Results

3.1. Histopathological examination

The results of the histopathological examinations for all compounds are summarized in Table 2. The high-dose groups of 23 tubular toxicants (gentamicin sulphate, vancomycin hydrochloride, 2-bromoethylamine hydrobromide, phenylbutazone, cyclosporine A, thioacetamide, K17, triamterene, allopurinol, nitrofurantoin, ethionine, N-phenylanthranilic acid, cisplatin, phenacetin, puromycin aminonucleoside, lomustine, cyclophosphamide, carboplatin, hexachlorobenzene, captopril, enalapril, indomethacin, and doxorubicin hydrochloride) exhibited necrosis, degeneration, and/or regeneration of the renal tubules at one or more sacrifice time during chronic exposure (days 4, 8, 15, and 29). Among them, 10 compounds (gentamicin sulphate, vancomycin hydrochloride, phenylbutazone, cyclosporine A, thioacetamide, K17, triamterene, allopurinol, N-phenylanthranilic acid, and cisplatin) exhibited the histopathological findings at all sacrifice time points. Tubular damage caused by nitrofurantoin or ethionine was repaired by day 15 or 29. The other 11 compounds caused nephrotoxicities only after a long period of chronic exposure (2-bromoethylamine hydrobromide, phenacetin, puromycin aminonucleoside after day 8, lomustine after day 15, and cyclophosphamide, carboplatin, hexachlorobenzene, captopril, enalapril, indomethacin, and doxorubicin hydrochloride after day 29). Although 10 of the potential tubular toxicants did not cause necrosis, degeneration, or regeneration, 6 of these 10 compounds caused other histopathological findings, such as vacuolation, anisonucleosis, hyaline droplet, swelling, hypertrophy, eosinophilic body, and cytoplasmic granule.

The middle-dose groups of 14 of the 23 tubular toxicants (gentamicin sulphate, cyclosporine A, thioacetamide, K17, triamterene, allopurinol, nitrofurantoin, ethionine, N-phenylanthranilic acid, cisplatin, puromycin aminonucleoside, hexachlorobenzene, captopril, and enalapril) had histopathological findings. Triamterene and allopurinol had histopathological findings at all of the sacrifice time points. The tubular damage in the middle-dose groups of nitrofurantoin and ethionine was repaired after long-time chronic exposure, which is consistent with their high-dose groups. The other 10 compounds yielded histopathological findings only after long-time chronic exposure. Thioacetamide only had histopathological findings at day 15. Although low-dose groups of 19 of the 23 tubular toxicants had no histopathological findings, the low-dose groups of gentamicin sulphate, triamterene, puromycin aminonucleoside, and hexachlorobenzene had degeneration or regeneration in renal tubules and/or cortex. In the case of gentamicin sulphate, triamterene, and hexachlorobenzene, only one or two animals in a group of five animals had minimal/slight degeneration/regeneration in the renal tubules. The animal that had the histopathological findings was not used for the microarray experiment (in the case of triamterene). The low-dose group of puromycin aminonucleoside had slight degeneration ($n = 4/5$) and regeneration ($n = 2/5$) in the renal tubules on day 29. But, the animals did not have apparent necrosis findings or significant changes

in BUN/CRE. Therefore, we considered these findings to be negative.

3.2. Microarray data analysis

3.2.1. Gene selection and supervised classification

For statistical reliability and regulatory perspective to determine the most appropriate analytical methods for the large-scale toxicogenomics database, we examined three different types of classification strategies, SVM-RFE, SVM+IBMT, and PAM. As the result of 5-fold cross-validation (randomly divided samples), we achieved the sensitivity of each classifier of 94% (SVM-RFE; 99 probes), 93.8% (SVM+IBMT; 99 probes), and 90% (PAM; threshold = 5.4), when we allowed 10% of false positives (Supplementary figures). Although the SVM-RFE was expected to have the highest classification accuracy, the correspondence rate of the feature gene list selected by recursive feature elimination between the sub-training sets was smaller than for the other two algorithms. The SVM-RFE classifier appeared to be over-fitted to the training set, so that the selected genes were not robust and were inadequate to be used as the biomarkers. In contrast, the feature genes selected by SVM+IBMT and PAM were similar between different training datasets generated during 5-fold CV. The prediction accuracy of the SVM+IBMT classifier was better than the PAM classifier. Therefore, we selected SVM+IBMT as the gene selection and classification algorithm.

We also tested prediction accuracy using the external test set. The group of 23 compounds containing positive samples and the group of 18 compounds containing only negative samples were randomly divided into 5 subsets 100 times. An arbitrary subset was used as the external test set, and the remaining subsets were used as the training set. We summarized the prediction results and achieved a sensitivity of 94.7% (SVM-RFE; 62 probes), 90% (SVM+IBMT; 98 probes), and 85.7% (PAM; threshold = 10) with a selectivity of 90% (Supplementary figures). In all three algorithms, the prediction accuracies calculated by using the external test sets were decreased compared to the accuracies calculated by 5-fold CV randomly divided samples. In the latter case, the training set and the test set possibly shared samples of the same compounds, times, and doses, such that the estimated accuracy was inappropriately high. It is always desirable to calculate the prediction accuracy using an external test set.

We used the top 98 probes (92 genes) to construct the SVM+IBMT classifier, considering the prediction accuracy and to avoid over-fitting (Table 3). The prediction accuracy was almost saturated and not significantly decreased compared to the max value, the number of support vectors was adequately lowered, and the number of feature genes was substantially smaller than the number of samples to avoid over-fitting (Supplementary figures). Also, the feature gene list is long enough to interpret their biological relevance. The probes ranked below the top 98 were also induced in renal tubular injury and biologically relevant. But around the top 600 genes, the number of support vectors was gradually increased, which means that these genes provided no more or little information for classification and tended to be over-fitting. The whole feature genes ranking is provided in the Supplementary Table. In addition, we tested the classifiers constructed from well-established single-genetic biomarkers and found that the classifier constructed from the multiple feature genes had much better prediction accuracy (Supplementary figures).

3.2.2. The gene expression profile of the feature genes

Fig. 1 shows the expression profile of the top 98 probes (92 genes) described above. Each color represents the Z-score of the log-ratio to the mean expression value of the corresponding control samples. The Z-scores were calculated by dividing the log-ratio

Table 2
Summary of histopathological findings.

Compound	Toxicity class	Findings (renal tubule)	Low				Middle				High			
			4D	8D	15D	29D	4D	8D	15D	29D	4D	8D	15D	29D
Gentamicin sulphate		Necrosis; degeneration; regeneration	0	0	0	1	0	0	0	1	1	1	1	1
Vancomycin hydrochloride		Degeneration; regeneration	0	0	0	0	0	0	0	2	1	1	1	1
2-Bromoethylamine hydrobromide		Regeneration	0	0	0	0	0	0	2	2	2	1	1	1
Phenylbutazone		Regeneration	0	0	0	0	0	0	0	0	1	1	1	1
Cyclosporine A		Degeneration; regeneration	0	0	0	0	0	1	1	1	1	1	1	1
Thioacetamide		Regeneration	0	0	0	0	0	0	1	0	1	1	1	1
K17		Necrosis; degeneration; regeneration	0	0	0	0	0	0	1	1	1	1	1	1
Triamterene		Regeneration	0	0	0	1	1	1	1	1	1	1	1	1
Allopurinol	Tubular toxicant (direct/indirect)	Regeneration	0	0	0	0	1	1	1	1	1	1	1	1
Nitrofurantoin		Regeneration	0	0	0	0	1	1	0	0	1	1	0	0
Ethionine		Degeneration; regeneration	0	0	0	0	1	0	0	0	1	1	1	0
N-Phenylanthranilic acid		Regeneration	0	0	0	0	1	2	0	1	1	1	1	1
Cisplatin		Necrosis; degeneration; regeneration	0	0	0	0	0	0	1	1	1	1	1	1
Phenacetin		Regeneration	0	0	0	0	0	0	0	0	1	1	1	1
Puromycin aminonucleoside		Degeneration; regeneration	0	0	1	1	0	2	1	2	2	1	1	1
Lomustine		Degeneration; regeneration	0	0	0	0	0	0	0	2	0	0	1	1
Cyclophosphamide		Regeneration	0	0	0	0	0	0	0	0	0	0	0	1
Carboplatin		Degeneration	0	0	0	0	0	0	0	0	0	0	0	1
Hexachlorobenzene		Regeneration	0	0	2	1	0	0	2	0	0	2	2	1
Captopril		Regeneration	0	0	0	0	0	0	0	1	0	0	0	1
Enalapril		Necrosis; regeneration	0	0	0	0	0	0	0	1	0	0	0	1
Indomethacin		Regeneration	0	0	0	0	0	0	0	0	0	2	1	1
Doxorubicin hydrochloride		Necrosis; degeneration	0	0	0	0	0	0	0	0	0	0	0	1
Ethinyl estradiol		Vacuolization	0	0	0	2	0	0	2	2	0	0	0	2
Monocrotaline		Anisonucleosis; vacuolization	0	0	0	0	0	0	0	2	0	0	2	
Acetaminophen		No-findings	0	0	0	0	0	0	0	0	0	2	0	0
Cephalothin sodium		Cytoplasmic granule	0	0	0	2	0	0	2	2	0	2	2	2
Bucetin	Potential tubular toxicant	No-findings	0	0	0	0	0	0	0	0	0	0	0	0
Methyltestosterone		Hypertrophy	0	0	0	0	0	0	0	2	0	0	2	2
Rifampicin		Hyaline droplet; eosinophilic body	0	2	2	2	0	2	2	2	0	2	2	2
Imipramine hydrochloride		No-findings	0	0	0	0	0	0	0	0	0	0	0	0
Acetazolamide		No-findings	0	0	0	0	0	0	0	2	0	0	2	2
Caffeine		No-findings	0	0	0	0	0	0	0	0	0	0	0	0
Valproic acid		No-findings	0	0	0	0	0	0	0	0	0	0	0	0
Clofibrate		No-findings	0	0	0	0	0	0	0	0	0	0	0	0
Allyl alcohol		No-findings	0	0	0	0	0	0	0	0	0	0	0	0
Omeprazole		No-findings	0	0	0	0	0	0	0	0	0	0	0	0
Bromobenzene	Hepatotoxicant (non-nephrotoxicant)	No-findings	0	0	0	0	0	0	0	0	0	0	0	0
Ketoconazole		No-findings	0	0	0	0	0	0	0	0	0	0	0	0
Ciprofloxacin		No-findings	0	0	0	0	0	0	0	0	0	0	0	0
Erythromycin ethylsuccinate		No-findings	0	0	0	0	0	0	0	0	0	0	0	0

The absence or presence of renal tubular toxicity is indicated as 0 or 1 according to the following findings: necrosis, degeneration, and regeneration. Other histopathological findings, such as tubular vacuolation, hypertrophy, or intracytoplasmic hyaline droplet, are indicated as 2.

Table 3
Top 98 probes (92 genes) ranked by Intensity-Based Modified T-statistics.

Function	Rank	IBMT-value	Probe ID	Gene symbol	Gene title
Tissue remodeling	67	16.58035006	1368419_at	Cp	Ceruloplasmin
	53	17.38025275	1367655_at	Tmsb10	Thymosin, beta 10
	42	18.32495826	1368418_a_at	Cp	Ceruloplasmin
	35	18.71625959	1370511_at	Fgb	Fibrinogen, B beta polypeptide
	34	18.75582061	1370992_a_at	Fga	Fibrinogen, alpha polypeptide
	25	19.4777112	1368160_at	Igfbp1	Insulin-like growth factor binding protein 1
	23	20.04881639	1387011_at	Lcn2	Lipocalin 2
	5	23.34760498	1367581_a_at	Spp1	Secreted phosphoprotein 1
	4	24.99287138	1367784_a_at	Clu	Clusterin
	3	25.55598409	1368420_at	Cp	Ceruloplasmin
	2	27.31956855	1367712_at	Timp1	Tissue inhibitor of metallopeptidase 1
	1	32.37802533	1387965_at	Havcr1	Kidney injury molecule 1
Immune response/inflammatory response	95	15.48262595	1367850_at	Fcgr3	Fc receptor, IgG, low affinity III
	85	15.87707814	1367786_at	Psmb8	Proteosome (prosome, macropain) subunit, beta type 8
	82	15.95556487	1370892_at	C4-2	Complementcomponent4a
	57	17.08681361	1368490_at	Cd14	CD14 antigen
	49	17.46443444	1379889_at	Lamc2	Laminin, gamma 2
	36	18.6392526	1367794_at	A2m	Alpha-2-macroglobulin
	31	19.03400005	1374033_at	Psmb10	Proteasome (prosome, macropain) subunit, beta type 10
	26	19.3233011	1374119_at	Elf3	E74-like factor 3
	21	20.17343592	1368921_a_at	Cd44	CD44 antigen
	12	20.92295884	1367614_at	Anxa1	Annexin A1
	10	21.33883134	1379340_at	Lamc2	Laminin, gamma 2
	7	22.90158183	1387952_a_at	Cd44	CD44 antigen
Cell adhesion/proliferation/migration	68	−16.55652999	1368131_at	Capn6	Calpain 6
	89	−15.74490892	1372869_at	Gtpbp4	GTPbindingprotein4
	98	−15.44895153	1370144_at	Gtpbp4	GTPbindingprotein4
	59	16.9871558	1367574_at	Vim	Vimentin
	56	17.09543212	1388587_at	Ier3	Immediate early response 3
	50	17.46375719	1367914_at	Emp3	Epithelial membrane protein 3
	47	17.49603392	1370177_at	PVR	Poliovirus receptor
	45	17.78791131	1388802_at	Bex1	Brain expressed X-linked 1
	40	18.45920696	1368612_at	Itgb4	Integrin beta 4
	32	18.86869018	1375170_at	S100a11	S100 calcium binding protein A11 (calizzarin)
	20	20.20478694	1373421_at	Tgif	TG interacting factor
	19	20.41704079	1386879_at	Lgals3	Lectin, galactose binding, soluble 3
	18	20.63006692	1371785_at	Tnfrsf12a	Tumor necrosis factor receptor superfamily, member 12a
	16	20.67075085	1386890_at	S100a10	S100 calcium binding protein A10 (calpactin)
	14	20.72852871	1368187_at	Gpnmb	Glycoprotein (transmembrane) nmb
Membrane transport	70	−16.51359077	1388097_at	Cacng5	Calcium channel, voltage-dependent, gamma subunit 5
	94	15.49715091	1380909_at	–	Transcribed locus
	73	16.25219965	1368497_at	Abcc2	ATP-binding cassette, sub-family C (CFTR/MRP), member 2
	9	22.17460015	1368168_at	Slc34a2	Solute carrier family 34 (sodium phosphate), member 2
Metabolism	93	15.55951107	1370813_at	Gstm5	Glutathione S-transferase, mu 5
	87	15.78307408	1372691_at	Upp1	Uridine phosphorylase 1
	65	16.68114127	1374070_at	Gpx2	Glutathione peroxidase 2
	61	16.95386475	1374784_at	Prtfdc1_predicted	Phosphoribosyl transferase domain containing 1 (predicted)
	44	17.95904453	1370561_at	A3galt2	Alpha-1,3-galactosyltransferase 2 (isoglobotriaosylceramide synthase)
	39	18.4925478	1370445_at	Pspla1	Phosphatidylserine-specific phospholipase A1
	33	18.84407902	1387925_at	Asns	Asparagine synthetase
Apoptosis	84	15.89635722	1370113_at	Birc3	Baculoviral IAP repeat-containing 3
	75	16.23159672	1368308_at	Myc	Myelocytomatosis viral oncogene homolog (avian)
Signal transduction	38	−18.53296844	1370522_at	Gcgr	Glucagon receptor
	69	16.51817598	1390510_at	Ms4a6b	Membrane-spanning 4-domains, subfamily A, member 6B
Angiogenesis/fibrinolysis	30	19.03449106	1367584_at	Anxa2	Annexin A2
Blood coagulation	52	17.3941316	1368052_at	Tspan8	Tetraspanin 8
Cell–cell communication	81	16.08958043	1388547_at	Cldn4	Claudin 4

Table 3 (*Continued*)

Function	Rank	IBMT-value	Probe ID	Gene symbol	Gene title
Detection of temperature stimuli	15	20.67755397	1367768_at	Lxn	Latexin
DNA replication initiation	97	15.47163164	1372406_at	LOC367976	Minichromosomemaintenancedeficient3 (S.cerevisiae)(predicted)
Endocytosis	80	16.0961982	1392648_at	Mrc1_predicted	Mannose receptor, C type 1 (predicted)
Kidney development	78	16.13533388	1368223_at	Adamts1	A disintegrin-like and metallopeptidse (reprolysin type) with thrombospondin type 1 motif, 1
Microtubule-based process	71	16.33428851	1387892_at	Tubb5	Tubulin, beta 5
miRNA-mediated gene silencing	88	15.75295308	1371583_at	Rbm3	RNA binding motif protein 3
rRNA processing	24	19.83460167	1373499_at	Gas5	Growth arrest specific 5
Stress fiber formation	58	17.05771651	1373286_at	Fblim1	Filamin binding LIM protein 1
Structural constituent of cytoskeleton	86	15.805369	1370288_a_at	Tpm1	Tropomyosin 1, alpha
	92	15.57704782	1382590_at	RGD1563347_predicted	Similar to RIKEN cDNA 2310015N21 (predicted)
	79	16.12099714	1376877_at	Cdcp1_predicted	CUB domain containing protein 1 (predicted)
	77	16.15247506	1368207_at	Fxyd5	FXYD domain-containing ion transport regulator 5
	62	16.9053337	1390226_at	RGD1562552_predicted	Similar to hypothetical protein LOC340061 (predicted)
	55	17.14203525	1389659_at	RGD1565540_predicted	Similar to ctla-2-beta protein (141 AA) (predicted)
	51	17.42187372	1393240_at	Efemp2	EGF-containing fibulin-like extracellular matrix protein 2
	29	19.0788577	1393643_at	Rcn1_predicted	Reticulocalbin 1 (predicted)
	28	19.09794144	1383401_at	LOC500040	Similar to Testis derived transcript
	13	−20.76507248	1390847_at	Tmem86a_predicted	Transmembrane protein 86A (predicted)
ESTs	17	−20.6670163	1373309_at	Tmem86a_predicted	Transmembrane protein 86A (predicted)
	96	−15.4719928	1374167_at	LOC361399	Similar to autoantigen
	90	15.72117787	1388340_at	Ns5atp9	NS5A (hepatitis C virus) transactivated protein 9
	83	15.92546837	1375224_at	Phlda3	Pleckstrin homology-like domain, family A, member 3
	72	16.3017568	1373035_at	–	–
	66	16.62012551	1390109_at	–	–
	64	16.80319643	1373908_at	–	–
	60	16.96481687	1371782_at	Nipsnap3a	Nipsnap homolog 3A (C. elegans)
	54	17.20576139	1373504_at	Glipr1	GLI pathogenesis-related 1 (glioma)
	43	17.9919912	1379957_at	Slfn8	Schlafen 8
	27	19.2586905	1388900_at	RGD1566118_predicted	RGD1566118 (predicted)
	22	20.17177219	1390839_at	Pqlc3	PQ loop repeat containing 3
	41	−18.40682675	1372911_at	–	Transcribed locus
	46	−17.76332084	1376913_at	–	Transcribed locus
	91	−15.59722933	1378292_at	–	Transcribed locus
	76	16.20156037	1385190_at	–	Transcribed locus
	74	16.23557955	1377994_at	–	Transcribed locus
	63	16.82551948	1397769_at	–	Transcribed locus
	48	17.48169748	1393252_at	–	Transcribed locus
	37	18.59863244	1376109_at	–	Transcribed locus
	11	20.9365083	1377092_at	–	Transcribed locus
	8	22.29041324	1391106_at	–	Transcribed locus
	6	23.16631514	1390659_at	–	Transcribed locus

values by the variance of the log-ratio value of the control samples calculated for each arbitrary range of the expression values. Then, the expression values of the control samples were pooled for each compound and time point ($n = 3$). Among the 92 genes, 83 genes were significantly up-regulated, and 9 genes were down-regulated in most of the positive samples (Fig. 1, Table 3). Most of the genes involved in tissue remodeling, the immune/inflammatory response, cell adhesion/proliferation/migration, and metabolism were up-regulated. Several up-regulated genes were also involved in membrane transport, signal transduction, apoptosis, and some of the other genes that were probably related to reconstruction of the kidney tissues (e.g., structural constituent of cytoskeleton). In particular, genes involved in tissue remodeling and the

immune/inflammatory response had many well-known biomarker candidates for renal tubular injury, as described by Wang et al. (2008) (8/10 and 2/10, respectively). Down-regulated genes participated in cell adhesion/proliferation/migration, membrane transport, and signal transduction.

Most of the 10 genes that participated in tissue remodeling were strongly up-regulated (Z-score > 2.5) in most of the positive samples (Fig. 1a). On day 4, a lot of genes already had been up-regulated after treatment with vancomycin hydrochloride, 2-bromoethylamine hydrobromide, phenylbutazone, cyclosporine A, thioacetamide, K17, triamterene, allopurinol, ethionine, N-phenylanthranilic acid, cisplatin, phenacetin, captopril, enalapril, and indomethacin. With the exceptions of 2-bromoethylamine
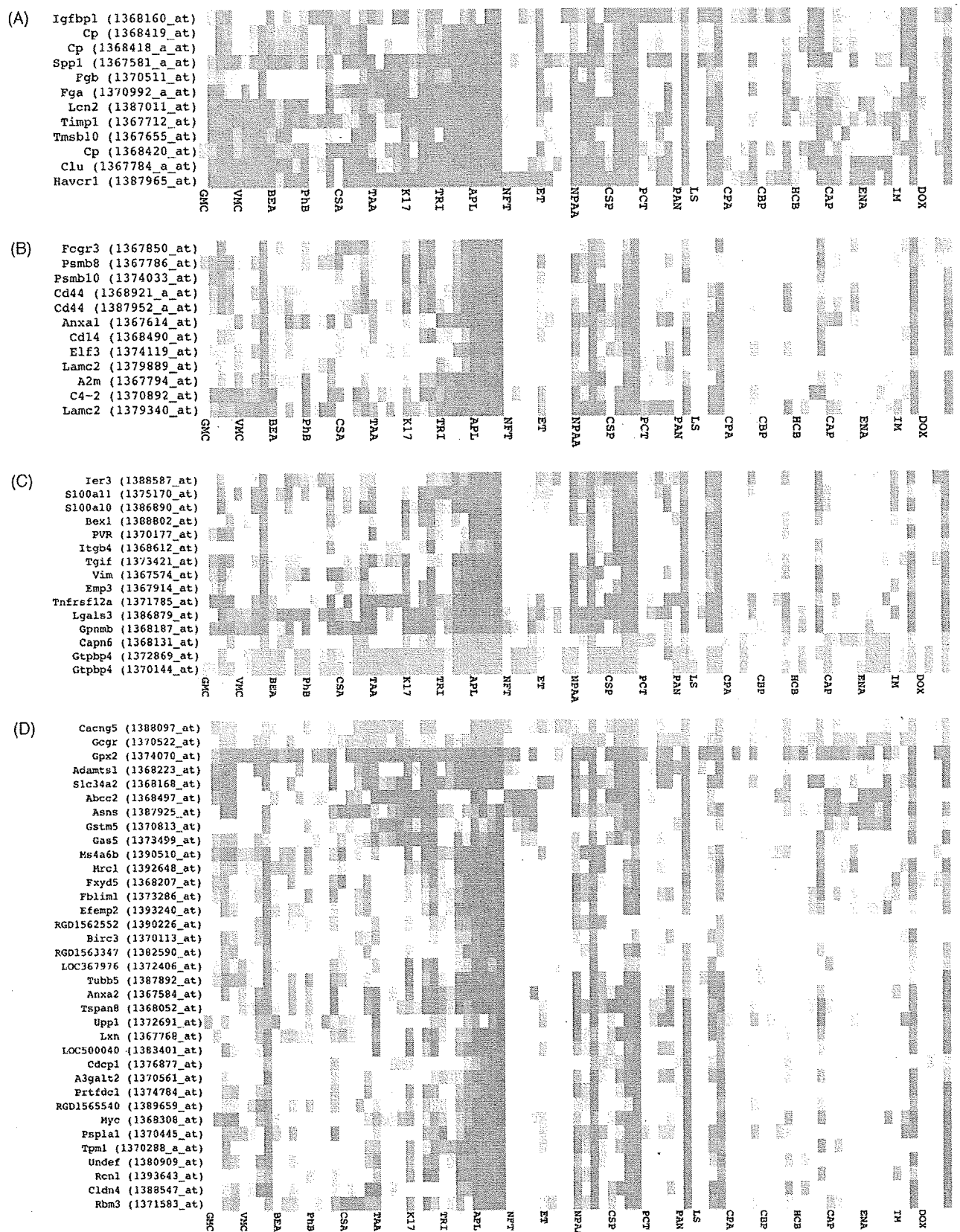
Fig. 1. The gene expression profile of the feature genes. Rows – genes, columns – sample groups. Each color represents the Z-score of the log-ratio to the mean expression value of the corresponding control samples (same compound and time point). Up-regulated genes (Z-score $\geq$ 2.5) are represented by red colors, and down-regulated genes (Z-score $\leq$ −2.5) are represented by blue colors. Each sample group is labeled with the compound abbreviation on day 4. The columns of each compound are ordered in time (from day 4 to day 29). (a) Tissue remodeling, (b) immune/inflammatory response, (c) cell adhesion/proliferation/migration, and (d) the others (membrane transport, metabolism, signal transduction, apoptosis). (For interpretation of the references to color in this figure legend, the reader is referred to the web version of the article.)

hydrobromide, phenacetin, captopril, enalapril, and indomethacin, histopathological findings had been observed in the animals treated with the above 10 compounds on day 4 (Table 2). In the case of 2-bromoethylamine hydrobromide, phenacetin, captopril, enalapril, and indomethacin, the histopathological findings were observed after day 8; therefore, these feature genes had been up-regulated before histopathological changes (in 2-bromoethylamine hydrobromide, slight dilatation of the cortex was observed in 1 of 5 animals). The animals treated with gentamicin sulphate and nitrofurantoin had histopathological findings on day 4, but predominant up-regulation of tissue remodeling-related genes was not observed. Puromycin aminonucleoside-, lomustine-, cyclophosphamide-, carboplatin-, hexachlorobenzene-, and doxorubicin hydrochloride-treated samples had neither histopathological findings nor induction of tissue remodeling-related genes on day 4 (in puromycin aminonucleoside, a slight hyaline droplet in the cortex was observed in 1 of 5 animals). Although, except for puromycin aminonucleoside, predominant up-regulation of the feature genes related to tissue remodeling was observed before the histopathological changes. On the other hand, nitrofurantoin-treated animals did not exhibit predominant induction of the genes at any of the time points examined. Ethionine-treated animals had histopathological findings on day 4, but recovered from pathological status on day 15, which is the same as nitrofurantoin-treated animals. In contrast to nitrofurantoin, predominant up-regulation was found in the animals treated with ethionine on days 4, 8, and 15, but the up-regulated genes gradually decreased in a time-dependent manner. While some of the feature genes were also up-regulated in some of the negative samples, the extent of up-regulation of these genes was weak compared to those in the high-dose groups of the positive compounds.

Although the immune/inflammatory response-related genes were not universally induced in the positive samples as compared to tissue-remodeling related genes, predominant up-regulation was observed in most of the positive compounds (Fig. 1b). The animals treated with 2-bromoethylamine hydrobromide exhibited predominant up-regulation on day 4, and some of the genes were up-regulated in phenacetin, captopril, and indomethacin before histopathological changes in a similar manner seen in tissue remodeling. nitrofurantoin- and enalapril-treated animals did not exhibit predominant up-regulation of the genes at any of the time points. In the case of thioacetamide and ethionine, predominant up-regulation was only found on day 4, despite the histopathological findings observed after day 4.

Among the 14 cell adhesion/proliferation/migration-related genes, 2 genes were predominantly down-regulated, and 12 genes were predominantly up-regulated in most of the positive compounds (Fig. 1c). In 2-bromoethylamine hydrobromide, cyclophosphamide, hexachlorobenzene, captopril, enalapril, indomethacin, and doxorubicin hydrochloride, some of the feature genes were induced before histopathological changes. In nitrofurantoin and ethionine, some of the feature genes were induced after histopathological findings disappeared. *Gtpbp4* (*GTP-binding protein 4*) was down-regulated in most of the positive compounds and up-regulated in a lot of negative compounds.

Genes in other functional categories were also induced (Fig. 1d). Seven genes related to metabolism were up-regulated. Among them, *Gpx2* (*glutathione peroxidase 2*) was not only up-regulated in most of the positive compounds, but also in some of the negative compounds. The other xenobiotic metabolic enzyme, *Gstm5* (*glutathione S-transferase, mu 5*), was not induced in some of the positive compounds. Most of the genes related to metabolism (probably involved in secondary compensatory mechanism of cell toxicity) were strongly up-regulated in the positive compounds that exhibited histopathological findings throughout chronic administration. On the other hand, *Asns* (*asparagines*

synthetase) was also induced in nitrofurantoin, thioacetamide, captopril, and enalapril, which exhibited histopathological findings only at the beginning or after long-term administration. *Abcc2* (*ATP-binding cassette, sub-family C, member 2*), which act as a multi-drug transporter, was also up-regulated in nitrofurantoin, thioacetamide, captopril, and enalapril. But, these two genes were also predominantly induced in the negative compounds (clofibrate or omeprazole). In summary, the same as for the other functional categories, the late-onset compounds (e.g., cyclophosphamide, captopril, enalapril) did not tend to predominantly induce the genes of the above functional categories at the early stage of administration, and the recovered compounds (e.g., 2-bromoethylamine hydrobromide, nitrofurantoin, and ethionine) did not induce these genes at the late stage. It seems that the expression profiles of the feature genes were not necessarily correlated to the severity of the histopathological findings at the time point; rather, they were correlated to the time-dependent profile of histopathological changes.

3.2.3. Prediction of the external test compounds

Middle-dose groups of all 41 compounds and high-dose groups of 10 compounds (and also high-dose groups of the remaining 31 compounds at the time points without histopathological findings), which had not been used as the training set, were used as the test set for further external validation of the classifier. As a result, 11 of 14 (78.5%) compounds of the middle-dose groups with histological lesions were correctly classified into the positive group of renal tubular injury, when we used SVM positive probability of 0.5 as the threshold (Table 4). Among them, captopril and enalapril exhibited predominant induction of tissue remodeling-related genes and some of the other genes (e.g., *Gtpbp4*, *Gpx2*, *Abcc2*) and were predicted as positive before any signs of tubular damage had occurred. The middle-dose group of LS on day 29 was classified into the positive group without the presence of tubular damage (the high-dose groups of the compound exhibited tubular damage). On the other hand, allopurinol, nitrofurantoin, and *N*-phenylanthranilic acid, which had histopathological findings at the middle-dose groups, were classified into the negative group. Although, in the case of allopurinol and *N*-phenylanthranilic acid, many feature genes were induced and had comparatively higher SVM probabilities.

Among 23 tubular toxicants, the high-dose groups of 11 compounds exhibited late onset of the histopathological findings. Seven of these 11 compounds (63.6%) were predicted as positive before histopathological changes (2-bromoethylamine hydrobromide, phenacetin, carboplatin, hexachlorobenzene, captopril, enalapril, and indomethacin). We also calculated SVM probabilities for the high- and middle-dose groups of 10 potential tubular toxicants and predicted 5 of the 10 compounds as positive (ethinyl estradiol, monocrotaline, acetaminophen, imipramine hydrochloride, and acetazolamide). In most of the compounds predicted as positive without histopathological findings at the early stage of drug-administration or at the lower dosage, a lot of feature genes of most of the functional categories had been already induced (especially tissue remodeling).

4. Discussion

In the present study, we identified 98 genomic biomarker candidates (92 genes) and successfully constructed a highly accurate classifier for the concurrent diagnosis of renal tubular injury using diverse groups of nephrotoxicants and hepatotoxicants. We first compared different types of gene selection and classification algorithms to select the best analytical methods (SVM+IBMT; Supplementary figures). Then, the external test sets were randomly generated 100 times to validate the classifiers. Most of the previous reports that executed a toxicogenomics analysis of renal tubular

Table 4
Histopathological findings and the result of the prediction of the further external test set.

Compound	Toxicity class	SVM positive probability											
		Low				Middle				High			
		4D	8D	15D	29D	4D	8D	15D	29D	4D	8D	15D	29D
Gentamicin sulphate		0.007	0.017	0.144	0.088	0.012	0.067	0.391	1.000	0.121	1.000	1.000	1.000
Vancomycin hydrochloride		0.002	0.003	0.006	0.008	0.004	0.003	0.006	0.036	0.929	0.901	1.000	1.000
2-Bromoethylamine hydrobromide		0.024	0.015	0.020	0.010	0.039	0.103	0.024	0.023	0.996	0.853	0.996	0.879
Phenylbutazone		0.054	0.029	0.066	0.015	0.064	0.062	0.115	0.020	0.996	0.524	0.872	1.000
Cyclosporine A		0.015	0.045	0.053	0.035	0.129	0.887	0.857	0.990	0.992	1.000	1.000	1.000
Thioacetamide		0.057	0.030	0.014	0.027	0.348	0.176	0.680	0.848	1.000	0.992	1.000	1.000
K17		0.006	0.308	0.148	0.035	0.320	0.107	0.996	0.992	1.000	1.000	1.000	1.000
Triamterene		0.044	0.016	0.006	0.013	0.581	0.046	0.947	0.721	1.000	0.991	1.000	1.000
Allopurinol		0.005	0.003	0.018	0.050	0.068	0.417	0.025	0.244	1.000	1.000	1.000	1.000
Nitrofurantoin		0.040	0.003	0.013	0.018	0.018	0.005	0.021	0.064	0.328	0.179	0.192	0.906
Ethionine		0.095	0.040	0.038	0.018	0.819	0.030	0.046	0.028	0.983	0.460	0.164	0.040
N-Phenylanthranilic acid	Tubular toxicant (direct/indirect)	0.076	0.030	0.040	0.035	0.032	0.164	0.128	0.400	1.000	1.000	1.000	1.000
Cisplatin		0.013	0.097	0.010	0.109	0.044	0.433	0.910	0.996	0.966	0.931	1.000	1.000
Phenacetin		0.005	0.006	0.027	0.004	0.008	0.011	0.034	0.012	0.688	1.000	1.000	1.000
Puromycin aminonucleoside		0.007	0.028	0.028	0.098	0.015	0.024	1.000	1.000	0.418	1.000	NA	NA
Lomustine		0.012	0.048	0.101	0.011	0.015	0.022	0.287	0.721	0.007	0.155	NA	NA
Cyclophosphamide		0.009	0.061	0.032	0.008	0.044	0.024	0.009	0.014	0.044	0.132	0.152	0.919
Carboplatin		0.006	0.014	0.020	0.009	0.007	0.046	0.116	0.277	0.046	0.331	0.600	1.000
Hexachlorobenzene		0.010	0.011	0.098	0.536	0.058	0.174	0.121	1.000	0.027	0.300	0.743	1.000
Captopril		0.004	0.015	0.063	0.031	0.028	0.552	0.639	0.953	0.970	0.967	0.910	0.959
Enalapril		0.039	0.343	0.066	0.064	0.058	0.423	0.920	0.674	0.307	0.958	0.574	0.972
Indomethacin		0.069	0.004	0.004	0.011	0.053	0.013	0.029	0.061	0.661	0.910	1.000	NA
Doxorubicin hydrochloride		0.008	0.015	0.013	0.025	0.010	0.022	0.009	0.018	0.004	0.021	0.025	1.000
Ethinyl estradiol		0.048	0.069	0.108	0.138	0.252	0.079	0.612	0.605	0.640	0.191	0.642	0.668
Monocrotaline		0.004	0.018	0.019	0.051	0.011	0.116	0.218	0.864	0.044	0.986	1.000	NA
Acetaminophen		0.026	0.039	0.011	0.042	0.021	0.185	0.019	0.365	0.458	0.143	0.932	0.981
Cephalothin sodium		0.011	0.013	0.009	0.008	0.109	0.008	0.006	0.042	0.143	0.047	0.060	0.120
Bucetin	Potential tubular toxicant	0.005	0.007	0.024	0.023	0.019	0.016	0.003	0.035	0.007	0.030	0.119	0.038
Methyltestosterone		0.024	0.011	0.001	0.005	0.003	0.004	0.006	0.011	0.005	0.030	0.081	0.170
Rifampicin		0.014	0.017	0.004	0.008	0.007	0.024	0.010	0.090	0.224	0.052	0.060	0.317
Imipramine Hydrochloride		0.016	0.009	0.027	0.018	0.022	0.012	0.068	0.002	0.022	0.104	0.547	0.118
Acetazolamide		0.049	0.034	0.017	0.011	0.049	0.586	0.098	0.035	0.039	0.209	0.192	0.159
Caffeine		0.007	0.008	0.011	0.005	0.003	0.011	0.006	0.014	0.047	0.019	0.016	0.021
Valproic acid		0.002	0.003	0.026	0.006	0.007	0.011	0.029	0.008	0.020	0.041	0.056	0.016
Clofibrate		0.034	0.032	0.007	0.006	0.026	0.017	0.007	0.024	0.158	0.022	0.077	0.072
Allyl alcohol		0.004	0.010	0.015	0.008	0.004	0.017	0.006	0.004	0.003	0.031	0.006	0.013
Omeprazole		0.007	0.015	0.036	0.032	0.032	0.244	0.079	0.008	0.011	0.036	0.136	0.052
Bromobenzene	Hepatotoxicant	0.006	0.004	0.005	0.007	0.019	0.007	0.039	0.009	0.005	0.007	0.039	0.026
Ketoconazole		0.004	0.004	0.012	0.003	0.007	0.004	0.011	0.007	0.022	0.009	0.015	0.010
Ciprofloxacin		0.008	0.009	0.007	0.026	0.007	0.015	0.009	0.012	0.010	0.003	0.007	0.020
Erythromycin ethylsuccinate		0.006	0.013	0.025	0.020	0.009	0.018	0.045	0.083	0.054	0.025	0.073	0.113

injury did not use an external test set or used only one external test set. These approaches were not statistically robust or biologically appropriate, because the prediction accuracy was possibly differentiated and deviated depending on how the whole dataset was split into the external test set and the training set. Because we used a variety of compounds, it was especially important to randomize the external test set for our analysis to avoid statistical deviations. Furthermore, we validated their prediction accuracies using middle-dose groups of all 41 compounds and the high-dose groups of 23 compounds that were not used in the training of the classifier. The classifier constructed by the genomic signatures exhibited a higher sensitivity than the histopathological findings in detecting renal tubular damage at lower doses and at earlier time points (Table 4). Our large-scale, high-quality toxicogenomics database and algorithms for gene selection and classification have higher statistical power than any of the previous studies and are very useful for robust biomarker selection and the prediction of drug-induced toxicities.

The feature genes that could be biomarker candidates for drug-induced renal tubular injury include several well-known biomarker candidate genes, such as *Kim1*, *Cp*, *Clu*, *Timp1*, and *Spp1*. We also identified several genes that were not frequently reported in previous studies but are included in functional categories thought to be mechanistically related to tubular toxicity, and the expression levels of these genes were correlated to the severity of the histopathological findings (Fig. 1). Wang et al. (2008) recently conducted a literature survey to collect tubular injury biomarkers that were described in multiple published studies, and they validated these biomarkers by using RT-PCR. Our gene list contains 11 of 24 validated genes (Table 3). Among the 11 genes, 8 genes are involved in tissue remodeling, and 2 genes are involved in the immune/inflammatory response. All of tissue remodeling and immune/inflammatory response-related genes were up-regulated, as described in the previous studies. These genes are thought to be related to secondary compensatory mechanisms of renal tubular injury (Huang et al., 2001). Eight of 10 tissue remodeling-related genes were consistent with the genes reported by Wang et al., and most of these genes were strongly up-regulated in most of the positive samples. The genes that participated in these two functional categories were strongly suggested as genomic biomarker candidates for drug-induced renal tubular injury.

We found that the up-regulation of tissue remodeling and immune/inflammatory-related genes was most prominently induced and roughly consistent with or induced earlier than the histopathological findings (Fig. 1a and b). Up-regulated genes also participated in metabolism, cell adhesion/proliferation/migration, apoptosis, membrane transport, and signal transduction (Fig. 1c and d). Two xenobiotics metabolism-related genes (*Gpx2*, *Gstm5*) were up-regulated, probably in response to oxidative stress (Rokushima et al., 2008). *Asns* (*Asparagine synthetase*) is crucial for asparagine synthesis and may be important for progression through the G1 phase of the cell cycle (Hutson and Kilberg, 1994). *A3galt2* (*alpha-1,3-galactosyltransferase 2*) is involved in the synthesis of the isoglobo-series of glycosphingolipids, which are suggested to be involved in apoptosis. *Pspla1* (*phosphatidylserine-specific phospholipase A1*) stimulates histamine release and, therefore, may be involved in the inflammatory response (Hosono et al., 2001). Some membrane transporters including the multidrug transporter were up-regulated and probably are commonly induced by the toxicities of the diverse class of nephrotoxicants. Up-regulated genes related to cell adhesion/proliferation/migration and apoptosis also would be related to secondary compensatory mechanisms, the same as for genes related to tissue remodeling and the immune/inflammatory response. Several of these genes have been reported as genomic biomarkers of renal tubular injury.

Down-regulated genes participated in cell adhesion/proliferation/migration, membrane transport, and signal transduction (Fig. 1c and d). The down-regulation may be a response to drug-induced toxicity or an adverse effect and may serve to maintain a low cellular energy status to minimize further damage (Safirstein et al., 1990). Down-regulation occurs during the acute phase of tubular damage induced by nephrotoxicants and acute ischemic renal injury (Amin et al., 2004; Hu et al., 2000; Huang et al., 2001). Representative down-regulated genes observed in our analysis were *Cacng5* (*calcium channel, voltage-dependent, gamma subunit 5*) and *Gcgr* (*glucagons receptor*). Calcium channels transport calcium ions in cell cytoplasm to the outside and maintain their gradient of concentration. Down-regulation of *Cacng5* may be a consequence of lower energy status or the perturbation of calcium homeostasis. Glucagons are peptide hormones that suppress glycolysis and accelerate gluconeogenesis. Therefore, down-regulation of *Gcgr* probably suppresses gluconeogenesis. Our results show that the down-regulation of energy-consuming processes is also observed in chronic renal tubular injury.

In summary, our results support previous studies that described correlations between well-known biomarker candidate genes or their functional categories and renal tubular injury. We used not only typical compounds that cause renal tubular injury but also a lot of compounds that have diverse effects and different patterns of histopathological changes with multiple time points and dosages. Our results suggest that well-known biomarkers and their functional categories for renal tubular injury are also induced by a wide variety of nephrotoxicants. On the other hand, we also found inconsistent and novel analytical results and heterogeneities between compounds that have different patterns of histopathological changes. It is thought that our gene list preferentially contains genes concerning secondary compensatory mechanisms rather than drug toxicity because of the diversity of the compounds used in our analysis. The feature genes were highly and commonly induced in the compounds, thus, the feature genes are highly statistically reliable and useful as genomic biomarkers during the drug-development process. On the other hand, it is also important to investigate the differences in gene expression profiles corresponding to the toxicity between diverse classes of compounds.

We used middle-dose groups and high-dose groups, which had not been used in the training set, as a further external test set for our classifier constructed from 98 top-ranked genomic biomarkers. Eleven of 14 compounds (78.5%) with histopathological findings at middle-dose groups were correctly classified as positive (Table 4). Also, some of these compounds were predicted as positive at the time points before the emergence of the tubular injury. These results indicate that genomic biomarkers are more sensitive than histopathological findings. On the other hand, although the middle-dose groups of allopurinol, nitrofurantoin, and *N*-phenylanthranilic acid exhibited histopathological findings, these compounds were predicted as negative. In the case of high- and middle-dose nitrofurantoin, renal tubular necrosis had been already observed within 24 h after administration (data not shown) and recovered after day 15. We found that most of our 98 genomic biomarker candidates were not significantly induced at the middle-dose groups of nitrofurantoin (Supplementary figure). Instead, the high-dose groups of nitrofurantoin exhibited gene expression changes in some of the 92 genes, and were predicted as positive (day 29). Therefore, it is thought that the gene expression profiles of middle-dose nitrofurantoin may reflect the recovery from tubular injury, even though the histopathological findings were still observed. In the case of *N*-phenylanthranilic acid, 3 of 5 animals sacrificed on day 29 did not exhibit any histopathological changes. In the case of allopurinol and *N*-phenylanthranilic

acid, many feature genes were induced and had comparatively higher SVM probabilities. These samples should be included in the training set to construct better classifiers, or heterogeneity may exist.

We also used the high-dose groups of 10 potential tubular toxicants as the test set. These compounds exhibited no histopathological findings of renal tubules (necrosis, degeneration, and regeneration), but the induction of renal tubular injury and/or other nephrotoxicities have been described in previous reports. Five of the 10 compounds (ethinyl estradiol, monocrotaline, acetaminophen, imipramine hydrochloride, and acetazolamide) were predicted as renal tubular injury positive. Monocrotaline- and ethinyl estradiol-treated animals had no tubular injury, and these compounds have not been reported as tubular toxicants. But, these compounds had anisonucleosis and/or vacuolization at cortex/proximal tubules. Acetaminophen was reported as a tubular toxicant. Therefore, it is reasonable that these three compounds were predicted as renal tubular toxicants. Imipramine hydrochloride- and acetazolamide-treated animals had no tubular injury, and these compounds have not been reported as tubular toxicants; thus, these may be false positives. However, in the high-dose group of imipramine hydrochloride on day 15, many of the feature genes, such as *Cp*, *Igfbp1*, *Fcgr3*, and *Cd14*, were induced. In the middle-dose group of acetazolamide on day 8, most of the genes related to tissue remodeling were strongly up-regulated, including *Kim1*, *Clu*, *Timp1*, *Cp*, and *Spp1*. Although these changes may reflect the early onset of nephrotoxicity, the possibility of false positives cannot be completely excluded.

The classifier constructed from multiple feature genes had much better prediction accuracy than classifiers constructed from any of the single or multiple well-known genomic biomarkers described above, histopathological findings, and any previous study (Fig. 3, Supplementary figure). Toxicogenomics and the large-scale database would be very useful in drug discovery and also helpful in risk estimation of nephrotoxicity. But, our analytical results suggest that there still exists unknown heterogeneity of gene expression between compounds that have different patterns of histopathological changes (times, severity, type of histopathological findings, etc.), even though the gene expression changes are concurrent with the histopathological findings. Also, further work is needed to adapt these genes into a toxicity screen by validating their reversibility and developing robust and convenient assays. We are now preparing experimental validation of our genomic biomarkers for concurrent diagnosis and gene expression analysis of further compounds. Accumulation of knowledge about various types of toxicities is very useful and important not only to identify specific biomarkers for an arbitrary toxicity, but also to understand mechanisms of drug-inducible toxicities.

Conflict of interest statement

The authors declare that there are no conflicts of interest.

Acknowledgements

Appendix A. Supplementary data

Supplementary data associated with this article can be found, in the online version, at doi:10.1016/j.tox.2009.09.003.

References

Amin, R.P., Vickers, A.E., Sistare, F., Thompson, K.L., Roman, R.J., Lawton, M., Kramer, J., Hamadeh, H.K., Collins, J., Grissom, S., Bennett, L., Tucker, C.J., Wild, S., Kind, C., Oreffo, V., Davis 2nd, J.W., Curtiss, S., Naciff, J.M., Cunningham, M., Tennant, R., Stevens, J., Car, B., Bertram, T.A., Afshari, C.A., 2004. Identification of putative gene based markers of renal toxicity. Environ. Health Perspect. 112, 465–479.

Battershill, J.M., 2005. Toxicogenomics: regulatory perspective on current position. Hum. Exp. Toxicol. 24, 35–40.

Fielden, M.R., Eynon, B.P., Natsoulis, G., Jarnagin, K., Banas, D., Kolaja, K.L., 2005. A gene expression signature that predicts the future onset of drug-induced renal tubular toxicity. Toxicol. Pathol. 33, 675–683.

Guyon, I., Weston, J., Barnhill, S., Vapnik, V., 2002. Gene selection for cancer classification using support vector machines. Mach. Learn. 46, 389–422.

Heinloth, A.N., Irwin, R.D., Boorman, G.A., Nettesheim, P., Fannin, R.D., Sieber, S.O., Snell, M.L., Tucker, C.J., Li, L., Travlos, G.S., Vansant, G., Blackshear, P.E., Tennant, R.W., Cunningham, M.L., Paules, R.S., 2004. Gene expression profiling of rat livers reveals indicators of potential adverse effects. Toxicol. Sci. 80, 193–202.

Hosono, H., Aoki, J., Nagai, Y., Bandoh, K., Ishida, M., Taguchi, R., Arai, H., Inoue, K., 2001. Phosphatidylserine-specific phospholipase A1 stimulates histamine release from rat peritoneal mast cells through production of 2-acyl-1-lysophosphatidylserine. J. Biol. Chem. 276, 29664–29670.

Hu, E., Chen, Z., Fredrickson, T., Gellai, M., Jugus, M., Contino, L., Spurr, N., Sims, M., Halsey, W., Van Horn, S., Mao, J., Sathe, G., Brooks, D., 2000. Identification of a novel kidney-specific gene downregulated in acute ischemic renal failure. Am. J. Physiol. Renal Physiol. 279, F426–F439.

Huang, Q., Dunn 2nd, R.D., Jayadev, S., DiSorbo, O., Pack, F.D., Farr, S.B., Stoll, R.E., Blanchard, K.T., 2001. Assessment of cisplatin-induced nephrotoxicity by microarray technology. Toxicol. Sci. 63, 196–207.

Hutson, R.G., Kilberg, M.S., 1994. Cloning of rat asparagine synthetase and specificity of the amino acid-dependent control of its mRNA content. Biochem. J. 304, 745–750.

Irwin, R.D., Boorman, G.A., Cunningham, M.L., Heinloth, A.N., Malarkey, D.E., Paules, R.S., 2004. Application of toxicogenomics to toxicology: basic concepts in the analysis of microarray data. Toxicol. Pathol. 32 (Suppl. 1), 72–83.

Jiang, Y., Gerhold, D.L., Holder, D.J., Figueroa, D.J., Bailey, W.J., Guan, P., Skopek, T.R., Sistare, F.D., Sina, J.F., 2007. Diagnosis of drug-induced renal tubular toxicity using global gene expression profiles. J. Transl. Med. 5, 47.

Perazella, M.A., 2005. Drug-induced nephropathy: an update. Expert Opin. Drug Saf. 4, 689–706.

Ransohoff, D.F., 2004. Rules of evidence for cancer molecular-marker discovery and validation. Nat. Rev. Cancer 4, 309–314.

Rokushima, M., Fujisawa, K., Furukawa, N., Itoh, F., Yanagimoto, T., Fukushima, R., Araki, A., Okada, M., Torii, M., Kato, I., Ishizaki, J., Omi, K., 2008. Transcriptomic analysis of nephrotoxicity induced by cephaloridine, a representative cephalosporin antibiotic. Chem. Res. Toxicol. 21, 1186–1196.

Safirstein, R., Price, P.M., Saggi, S.J., Harris, R.C., 1990. Changes in gene expression after temporary renal ischemia. Kidney Int. 37, 1515–1521.

Sartor, M.A., Tomlinson, C.R., Wesselkamper, S.C., Sivaganesan, S., Leikauf, G.D., Medvedovic, M., 2006. Intensity-based hierarchical Bayes method improves testing for differentially expressed genes in microarray experiments. BMC Bioinformatics 7, 538.

Searfoss, G.H., Ryan, T.P., Jolly, R.A., 2005. The role of transcriptome analysis in pre-clinical toxicology. Curr. Mol. Med. 5, 53–64.

Somorjai, R.L., Dolenko, B., Baumgartner, R., 2003. Class prediction and discovery using gene microarray and proteomics mass spectroscopy data: curses, caveats, cautions. Bioinformatics 19, 1484–1491.

Tibshirani, R., Hastie, T., Narasimhan, B., Chu, G., 2002. Diagnosis of multiple cancer types by shrunken centroids of gene expression. Proc. Natl. Acad. Sci. U.S.A. 99, 6567–6572.

Thukral, S.K., Nordone, P.J., Hu, R., Sullivan, L., Galambos, E., Fitzpatrick, V.D., Healy, L., Bass, M.B., Cosenza, M.E., Afshari, C.A., 2005. Prediction of nephrotoxicant action and identification of candidate toxicity-related biomarkers. Toxicol. Pathol. 33, 343–355.

Urushidani, T., Nagao, T., 2005. Toxicogenomics: the Japanese initiative. In: Borlak, J. (Ed.), Handbook of Toxicogenomics-Strategies and Applications. Wiley-VCH, Weinheim, pp. 623–631.

Vapkin, V., 1995. The Nature of Statistical Learning Theory. Springer-Verlag, New York, Inc.

Wang, E.J., Snyder, R.D., Fielden, M.R., Smith, R.J., Gu, Y.Z., 2008. Validation of putative genomic biomarkers of nephrotoxicity in rats. Toxicology 246, 91–100.

Reproductive and Developmental Toxicity Screening Study of 2,4-Dinitrophenol in Rats

Mika Takahashi,[1] Masao Sunaga,[2] Mutsuko Hirata-Koizumi,[1] Akihiko Hirose,[1] Eiichi Kamata,[1] Makoto Ema[1]

[1]Division of Risk Assessment, Biological Safety Research Center, National Institute of Health Sciences, Tokyo 158-8501, Japan

[2]Safety Research Institute for Chemical Compounds Co., Ltd., Sapporo 004-0839, Japan

ABSTRACT: Rats were treated by gavage once daily with 2,4-dinitrophenol (DNP) at 0 (control), 3, 10, or 30 mg/kg bw. Males were dosed for 46 days, beginning 14 days before mating, and females were dosed for 40–47 days, from 14 days before mating to day 3 of lactation. No deaths were observed in males and females of any group. A significant decrease in body weight gain and significant increase in liver weight were found in males and females at 30 mg/kg bw/day. The number of live pups on postnatal days (PNDs) 0 and 4, live birth index, and body weight of live male and female pups on PNDs 0 and 1 were significantly lowered at 30 mg/kg bw/day. External and internal examinations of pups revealed no increased incidence of malformations in DNP-treated groups. On the basis of these findings, we concluded that DNP has general and reproductive/developmental toxicity, but not teratogenicity, under the present conditions. The NOAEL of DNP is considered to be 10 mg/kg bw/day in rats. © 2008 Wiley Periodicals, Inc. Environ Toxicol 24: 74–81, 2009.

Keywords: 2,4-dinitrophenol; reproductive/developmental toxicity; rat

INTRODUCTION

2,4-Dinitrophenol (DNP; CAS No. 51-28-5) is one of the six different isomers of dinitrophenols, and the most commercially important isomer. Commercial dinitrophenol, a mixture of DNP and smaller amounts of 2,3- and 2,6-dinitrophenol, is used in the synthesis of picric acid and picramic acid, and for making dyes, wood preservatives, photographic developers, explosives, and insecticides (ATSDR, 1995). The production volume of DNP exceeded 1 million pounds/year in the U.S. (Scorecard, 2007) and was around 1000 tons in Japan in 2005 (METI, 2006). DNP is used for the same purposes as dinoseb, 2-sec-butyl-4,6-dinitrophenol, which was registered as a herbicide and insecticide.

DNP was once taken extensively as a weight reduction drug in the 1930s (Simkins, 1937a,b). Thereafter, adverse effects, including cataracts, renal damage, and death due to hyperthermia, were noted in people who took DNP (Beinhauer, 1934; Epstein and Rosenblum, 1935; Goldman and Haber, 1936; Simkins, 1937a,b). DNP was banned for use for this purpose by authorities in the U.S. in 1938 (Parascandola, 1974; Kurt et al., 1986); however, it can be still illicitly purchased in the U.S. as a diet pill via commercial web sites, and incidents, including deaths, have been reported (Miranda et al., 2006). DNP is released into the environment primarily during its manufacture and use, and from waste disposal sites that contain DNP (ATSDR, 1995), and can also form in the atmosphere from the reaction of benzene with NOx in ambient air (Nojima et al., 1983). General population and occupational exposures may occur primarily through the inhalation of ambient air (ATSDR, 1995). According to TRI01 (U.S. EPA, 2001), total on- and off-site release was around 100 000 pounds in